



โครงการการเรียนการสอนเพื่อเสริมประสบการณ์

ลักษณะจำเพาะของโครงสร้างรูปพรุนในหินทรายจากแอ่งพิษณุโลก

โดย

นางสาวชัตติยาภรณ์ ทิพย์รองพล

เลขประจำตัวนิสิต 5832703023

โครงการนี้เป็นส่วนหนึ่งของการศึกษาระดับปริญญาตรี
ภาควิชาธรณีวิทยา คณะวิทยาศาสตร์ จุฬาลงกรณ์มหาวิทยาลัย
ปีการศึกษา 2561

บทคัดย่อและแฟ้มข้อมูลฉบับเต็มของโครงการทางวิชาการที่ให้บริการในคลังปัญญาจุฬาฯ (CUIR)

เป็นแฟ้มข้อมูลของนิสิตเจ้าของโครงการทางวิชาการที่ส่งผ่านทางคณะที่สังกัด

The abstract and full text of senior projects in Chulalongkorn University Intellectual Repository (CUIR)
are the senior project authors' files submitted through the faculty.

ลักษณะจำเพาะของโครงสร้างรูพรุนในหินทรายจากแอ่งพิบูลย์โลก

นางสาวชัตติยาภรณ์ ทิพย์รองพล

โครงการนี้เป็นส่วนหนึ่งของการศึกษาตามหลักสูตรวิทยาศาสตรบัณฑิต

ภาควิชาธรณีวิทยา คณะวิทยาศาสตร์ จุฬาลงกรณ์มหาวิทยาลัย

ปีการศึกษา 2560

CHARACTERIZATION OF PORE STRUCTURE IN SANDSTONE FROM THE PHITSANULOK BASIN

Ms. Khattiyaporn Tiprongpon

A Project Submitted in Partial Fulfillment of the Requirements
for the Degree of Bachelor of Science Program in Geology
Department of Geology, Faculty of Science, Chulalongkorn University
Academic Year 2018

หัวข้อโครงการ	ลักษณะจำเพาะของโครงสร้างรูปพูนในหินทรายจากแอ่งพิชญโลก
โดย	นางสาวชัตติยาภรณ์ ทิพย์รองพล
สาขาวิชา	ธรณีวิทยา
อาจารย์ที่ปรึกษาโครงการหลัก	ผู้ช่วยศาสตราจารย์ ดร.วรัญทร คณิตปัญญาเจริญ

วันที่ส่ง 13 พฤษภาคม 2562

วันที่อนุมัติ 13 พฤษภาคม 2562



.....
 อาจารย์ที่ปรึกษาโครงการหลัก
 (ผู้ช่วยศาสตราจารย์ ดร.วรัญทร คณิตปัญญาเจริญ)

Project Title PROJECT TITLE CHARACTERIZATION OF PORE STRUCTURE
IN SANDSTONE FROM THE PHITSANULOK BASIN

By Miss Khattiyaporn Tiprongpon

Field of Study Geology

Project AdvisorAssistant Professor Dr.Waruntorn Kanitpanyacharoen

Submitted date 13 May 2019

Approval date 13 May 2019

Waruntorn

Project Advisor

(Assistant Professor Dr. Waruntorn Kanitpanyacharoen)

ชติยาภรณ์ ทิพย์รองพล : ลักษณะจำเพาะของโครงสร้างรูพรุนในหินทรายจากแอ่งพิชญ์โลก.
(CHARACTERIZATION OF PORE STRUCTURE IN SANDSTONE FROM THE PHITSANULOK
BASIN) อ.ที่ปรึกษาโครงการหลัก : ผู้ช่วยศาสตราจารย์ ดร.วรัญทร คณิตปัญญาเจริญ, 54 หน้า.

แหล่งกักเก็บปิโตรเลียมรูปแบบใหม่ได้รับความสนใจในการค้นหาแหล่งปิโตรเลียมเพิ่มขึ้น หินทรายเนื้อ
แน่นเป็นแหล่งกักเก็บปิโตรเลียมชนิดหนึ่งที่มีความนิยมเป็นอย่างมากในอุตสาหกรรมปิโตรเลียมเนื่องจากแสดง
ปริมาณการกักเก็บน้ำมันและแก๊ซธรรมชาติที่มีปริมาณมาก โครงสร้างจุลภาคของหินทรายเนื้อแน่นมีความยากใน
การศึกษาเนื่องจากขนาดตะกอนและขนาดรูพรุนที่เล็ก ค่าความพรุนต่ำ และช่องเชื่อมต่อรูพรุนมีความซับซ้อน
โครงสร้างจุลภาคและคุณสมบัติของหินชนิดนี้สามารถศึกษาได้ภายใต้เครื่องมือการวิเคราะห์ภาพตัดขวางด้วยรังสี
เอ็กซ์ซิงค์โครตรอน ที่แสดงรูปร่างสามมิติและมีความละเอียดสูง จากการศึกษาพบว่า ขนาดตะกอนในตัวอย่าง
PH1 PH2 และ PH3 คือ 61.15, 30.01, 41.11 ไมโครเมตร ซึ่งจัดอยู่ในทรายละเอียดมาก ทรายแป้งขนาดกลาง
และทรายแป้งขนาดหยาบ ลักษณะรูปร่างของรูพรุนประกอบไปด้วยสามประเภท คือรูพรุนระหว่างตะกอน รูพรุน
ที่มุมของตะกอนแข็ง และรอยแตกจุลภาค ซึ่งรอยแตกจุลภาคสามารถเพิ่มความสามารถในการไหลของของไหล
ได้มากที่สุด อัตราส่วนระหว่างความกว้างและความยาวของรูพรุนในสามมิติมีค่าน้อยกว่า 1 แสดงถึงรูปร่างที่แบน
และเป็นแท่งซึ่งมีขนาดใกล้เคียงกันในตัวอย่าง PH1 และ PH2 คือ 0.48 และ 0.47 ตามลำดับซึ่งส่งผลให้รูพรุนมี
รูปร่างเป็นทรงรีหรือรูปทรงไข่ ขณะที่ PH3 มีอัตราส่วนระหว่างความกว้างและความยาวในสามมิติที่ 0.35 ส่งผล
ให้รูพรุนมีรูปร่างค่อนข้างแบนและเป็นท้อ ค่าของช่องเชื่อมต่อรูพรุนมีขนาดในช่วง 0.36 ถึง 2.67 ไมโครเมตร มี
รูปร่างอยู่ในลักษณะทรงกลมและทรงรีมีขนาดที่สามารถเป็นแหล่งเก็บสะสมปิโตรเลียมได้และใกล้เคียงกับหิน
ทรายในอ่าวเท็กซัสตะวันออก รูปร่างของช่องเชื่อมต่อรูพรุนมีลักษณะเป็นแท่งและทรงรีเป็นส่วนใหญ่ ค่าความ
พรุนอยู่ในช่วงร้อยละ 9.41 ถึง 24.34 และค่าความสามารถในการซึมผ่านในช่วง 0.12 ถึง 0.49 มิลลิดาร์ซี ค่า
ความสามารถในการไหลที่ดีที่สุดในตัวอย่าง PH3 ส่งผลจากรูพรุนชนิดรอยแตก รูปร่างรูพรุนที่แบนและมีลักษณะ
เป็นท้อ ปริมาตรรูพรุนขนาดใหญ่มีปริมาณมาก และช่องเชื่อมต่อรูพรุนแบบท้อ และเส้นผ่านศูนย์กลางขนาดใหญ่
ของช่องเชื่อมต่อรูพรุน ขณะที่ในตัวอย่าง PH2 มีค่าการไหลน้อยที่สุด ส่งผลมาจากรูปร่างรูพรุนที่เชื่อมต่อกันน้อย
ปริมาตรรูพรุนขนาดเล็กมีปริมาณมาก รูปร่างของช่องเชื่อมต่อรูพรุนที่เป็นแผ่น และเส้นผ่านศูนย์กลางของช่อง
เชื่อมต่อรูพรุนมีขนาดเล็ก

ภาควิชาธรณีวิทยา	ลายมือชื่อนิสิต <i>ชติยาภรณ์ ทิพย์รองพล</i>
สาขาวิชา	ธรณีวิทยา	ลายมือชื่อ อ.ที่ปรึกษาหลัก..... <i>วรัญทร</i>
ปีการศึกษา	2561	ลายมือชื่อ อ.ที่ปรึกษาร่วม.....

5832703023 : MAJOR GEOLOGY

KEYWORDS : MICROSTRUCTURE / PORE SHAPE / POROSITY AND PERMEABILITY

KHATTIYAPORN TIPRONGPON : CHARACTERIZATION OF PORE STRUCTURE IN SANDSTONE FROM THE PHITSANULOK BASIN. ADVISOR : ASSISTANT PROFESSOR DR.WARUNTORN KANITPANYACHAROEN, Ph.D., 54 pp.

Tight sandstone has increasingly received interest as an unconventional reservoir in the petroleum industry due to its large oil and gas reserves. Microstructures of tight sandstone are difficult to be characterized because of their small grain sizes, low porosity, pore geometry, and pore throat. Complex microstructures and properties can be derived from advanced analytical tools as synchrotron X-ray tomography. Synchrotron X-ray experiments provide high spatial resolution of 3D information and nondestructive the samples. The average of grain size in PH1, PH2, and PH3 is 61.15, 30.01, 41.11 μm which are classified into very fine sand, medium silt, and coarse silt respectively. Three type of pore are observed in the samples which are pore between grains, pore at the edge of rigids grains and fracture pores. The 3D aspect ratio of pore in PH1 and PH2 are comparable,0.48 and 0.47 and suggesting oval shape of pore. In contrast the 3D aspect ratio in PH3 is 0.35 and show tabular and flat shape of pore. The diameter of pore throat in all samples are mostly spheroid and rod-like, ranging from 0.36 to 2.67 μm which is consistent with tight sandstone from other reservoirs such as Texas the greatest number of Basin. In addition, porosity range 9.41 to 24.34 % while permeability ranges from 0.12 to 0.49 mD. The highest permeability is PH3 which contains of the greatest number of fracture pores, tabular and flat pore shape from 3D aspect ratio, the number of high-volume pores, rod and spheroid pore throat, and the biggest size of average pore throat diameter. In contrast, the lowest permeability PH2 contains low connectivity of pore shape, low pore volume, plate like pore throat, and small pore throat diameter.

Department : Geology
Field of Study : Geology
Academic Year : 2018

Student's Signature..... *Khattiyaporn Tiprongpon*
Advisor's Signature..... *Waruntorn Kanitpanyacharoen*
Co-advisor's Signature..... —

Acknowledgement

I would like to express my very great appreciation to my research project supervisor Asst. Prof. Dr. Waruntorn Kanitpanyacharoen for her valuable and constructive suggestions during the planning and development of this research work. Her willingness to give her time so generously has been very much appreciated. My grateful thanks are also extended to our group project, Mr. Pitchaya Hotarapavanon, Mr. Thanyaboon Suthasirikul, Ms Ontima Yamchuti and Mr. Worapop Thongsame for their supporting and useful recommendation.

Finally, I wish to thank the entire department of Geology staff for supporting everything during this study.

Khattiyaporn Tiprongpon

Table of Contents

Acknowledgement	vi
Table of Contents	vii
Table of Figures	
List of Tables	iii
Chapter I Introduction and Literature Reviews	1
1.1 Introduction	1
1.2 Objectives	2
1.3 Literature reviews	2
1.3.1 <i>Unconventional Reservoir</i>	2
1.3.2 <i>Tight sandstone</i>	3
1.3.3 Pore Throat.....	5
1.3.4 <i>Micro-CT analysis</i>	7
Chapter II Study Area	8
2.1 Phitsanulok Basin.....	8
2.2 Regional Tectonic setting and Basin Evolution	9
2.3 Stratigraphy	12
2.4 Petroleum system.....	15
2.4.1 <i>Source rock</i>	15
2.4.2 <i>Reservoir</i>	16
2.4.3 <i>Seal</i>	17
2.4.4 <i>Trap</i>	17
Chapter III Methodology.....	19

3.1 Samples preparation.....	19
3.2 Data Analysis	20
Chapter IV Results.....	26
4.1 Grain Size Analysis.....	27
4.2 Pore Classification	29
4.3 3D Pore shape and Volume	32
4.4 Pore Throat.....	34
4.5 Porosity and Permeability.....	37
Chapter V Discussion and Conclusion	40
5.1 Porosity and Permeability.....	40
5.2 Pore Classification	41
5.4 Conclusion	44
References.....	45

Table of Figures

Figure 1.1 Unconventional reservoir fluid flow.	2
Figure 1.2 Worldwide hydrocarbon resources. Note conventional resources make up less than a third of the total	3
Figure 1.3 APEC's natural gas production (2011)	3
Figure 1.4 EIA assessments of shales gas and tight oil resources in Sichuan Basin, China (EIA,2016)	4
Figure 1.6 Pore throat is the small pore space at the point where two grains meet (Zhenpeng 2015)	6
Fig 1.7 Sizes of molecules and pore throats in siliciclastic rocks (Nelson,2009)	6
Figure 2.1 Location map of the Sirikit Field, Phitsanulok Basin, Thailand (C&C reservoirs, 2009)	8
Figure 2.2 Regional Tectonic setting of Thailand. (After Thai Shell Exploration and Production, 1988)	9
Figure 2.3 Structural model of Phitsanulok Basin (phase I & II) (After Thai Shell Exploration and Production, 1988)	11
Figure 2.4 Structural model of Phitsanulok Basin (phase III & IV) (After Thai Shell Exploration and Production, 1988)	12
Figure 2.5 Schematic S-N cross section of Sirikit Field shows the Stratigraphy Of Phitsanulok Basin. Lithostratigraphy comprises 8 units (After Thai Shell Exploration and Production, 1988)	13
Figure 2.6 Schematic depositional environment of Phitsanulok Basin. (After Thai Shell Exploration and Production, 1988)	14
Figure 2.7 Stratigraphy of the Phitsanulok Basin (C&C reservoirs, 2009)	14
Figure 2.8 HI versus OI plot of source rocks in Phitsanulok Basin. (Illustrated from Bal et al., 1992)	15
Figure 2.9 Marceral Analysis (Illustrated from Bal et al., 1992)	16
Figure 2.10 Fault sealing and trapping mode in Phitsanulok Basin. (Illustrated from Thai Shell Exploration and Production, 1988)	17

Figure 2.11 Fault sealing and trapping mode in Phitsanulok Basin. (Illustrated from Shell Exploration and Production, 1988)	18
Figure 3.1 Schematic diagram of the Synchrotron X-ray Micro-CT experiment. (Kanitpanyacharoen et al., 2013)	19
Figure 3.2 Beer-Lambert Law show that the light intensity come into the material has a different value with the light intensity throughout. (www.slideplayer.com)	20
Figure 3.3 Image before thresholding segmentation.	21
Figure 3.4 Different shades of grayscale was used to identify the material	22
Figure 3.5 Illustration of the selected single pore.	22
Figure 3.6 Flow simulation which is the results from permeability.	23
Figure 3.7 The binary image where one of the intensity levels equal to pore and one equal to the matrix in pore detection.	24
Figure 3.8 The analysis diameter histogram.	24
Figure 3.9 3D Simulation of Auto skeleton module.	25
Figure 4.1 Three sample of tight sandstone was divided into 3 area (Total 9 VOI) Sample PH1, PH2, and PH3 are a, b, and c respectively.	26
Figure 4.2 (a) The grey scale value from 0–65 thresholding scale represented pore-space while (b) 65–255 thresholding scale represented rock matrix.	27
Figure 4.3 Grain size classification which analyzed due to grain diameter (Wenworth, 1922)	28
Figure 4. 4 Grain size analysis classified by grain diameter based on Wenworth scale.	28
Figure 4.5 Pore shape classification (Louck et al.,2012)	30
Figure 4.6 Three pores type f in samples of this study (a) Pores between grains (b) Pores at the edge of rigid grains (c) Fracture pores	31
Figure 4.7 Width versus Length plot of pore in PH1, PH2, and PH3.	33
Figure 4.8 Pore Skeleton use to identify and calculate geometry of pore throat. (a) Cyan areas represent the whole pore space in sample after Auto Skeleton Module (b) Grey spheres represent the pore chamber and red skeleton represent the connectivity area of pore chamber (pore throat)	34

Figure 4.9 (a) 3D simulation of Pore Throat show the radius and length which can calculate the geometry of throat. (b) Grey spheres represent the pore chamber and red skeleton represent the connectivity area of pore chamber (pore throat)	35
Figure 4.10 This graph shows pore throat radius of PH1, Ph2, and PH3.	35
Table 4.1 Minimum, maximum, average radius of pore throat in PH1, PH2. And PH3.	36
Figure 4.12 Zingg diagram plot of l,L, S length of pore throat in PH1, PH2, and PH3.	38
Table 4.2 Porosity and Permeability of PH1, PH2, and PH3.	39
Figure 4.13 3D pore distribution in PH1, PH2, and PH3.	39
Figure 4.14 Porosity versus Permeability plot of 9 VOI	40
Figure 4.15 Sizes of pore throats in siliciclastic rocks on a logarithmic scale covering seven orders of magnitude. The res line shows then pore throat size ranges of 9 VOI of this study (Modified from Nelson,2009)	42
Figure 4.16 Grain size, pore size, and pore-throat size for 27 sandstone samples (Wardlaw and Cassan, 1979) The blue, red, and yellow line show the pore and pore throat of PH1, PH2, and PH3 respectively.	43
Figure 4.17 Flow simulation PH3 compare to PH2	44

List of Tables

Table 1.1 Test Description for pore structure characterization (Zhenpeng et al., 2015)	7
Table 4.1 Minimum, maximum, average radius of pore throat in PH1, PH2. And PH3	3
Table 4.2 Porosity and Permeability of PH1, PH2, and PH3	39

Chapter I

Introduction and Literature Reviews

1.1 Introduction

Tight sandstone has increasingly received interest as an unconventional reservoir in the petroleum industry due to its large oil and gas reserves (Zou et al., 2012). Tight sandstone reservoirs are defined with porosity and permeability values being less than 10% and 0.1 mD, respectively (Zou et al., 2012). Tight sandstone is considered as an unconventional reservoir because permeabilities of 0.1 md or less are officially recognized by the U.S. Federal Energy Regulatory Commission (AAPG Wiki). The unconventional reservoirs contain a wide variety of pore throat, ranging from sub-millimeter to nanometer (Nelson, 2009). Complex pore geometry and pore throat are the important factors, affecting the reservoir quality and fluid flow (Lai et al., 2018). The size of pore throat is generally 2 to 0.03 mm in tight gas sandstones (Nelson, 2009).

In addition, microstructures of tight sandstone are difficult to be characterized because of their small grain sizes, low porosity, pore geometry, and pore throat. Complex microstructures and properties can be derived from advanced analytical tools such as scanning electron microscope (SEM), transmission electron microscope (TEM), and synchrotron X-ray tomography. Synchrotron X-ray experiments provide high spatial resolution of 3D information, which is useful to visualize the pore geometry and pore connectivity as well as to understand the permeability and flow within the rocks (Zhenpeng et al., 2015). This study thus aims to investigate 3D microstructures, particularly pore structure and connectivity, of tight sandstones from the Phitsanulok Basin. Phitsanulok Basin, the largest onshore oil reservoir in Thailand, contains a large amount of tight sandstone such as K, L, M Formation in Lan Krabu Formation (Kiatrabile, 2016).

Tight sandstone in this area can produce kerogen type I, II, III, which have the potential to generate oil and gas (Kiatrabile, 2016). However, there is little research on the properties of tight sandstone reservoirs. To establish a better understanding of the relationship between pore geometry and flow ability, this research thus investigates pore system, which includes pore volume, pore throat, porosity, and permeability in tight sandstones from the Phitsanulok Basin.

1.2 Objectives

1.3.1 To quantify porosity and permeability in tight sandstones

1.3.2 To characterize pore shape, pore volume, and pore throat that affect the fluid flow and permeability

1.3 Literature reviews

1.3.1 Unconventional Reservoir

Unconventional reservoirs are the reservoir that have a low permeability and porosity so are difficult to produce. The difference between unconventional and conventional reservoir is conventional it is not be able to drill in the horizontal if we have the well vertically but, on the second hand we produce from the source in the unconventional condition so we must have a horizontal drilling, In the unconventional reservoir the gas and oil does not migrate from the source rock into the reservoir (Figure 1.1) To produce from unconventional reservoir has to create the fracturing network.

Only a third of worldwide oil and gas reserves are conventional, the remainder are in unconventional resources (Figure 1.2) The five major type of unconventional reservoirs are tight gas sandstone, coalbed methane, shale, Tar sand, Methane hydrate.

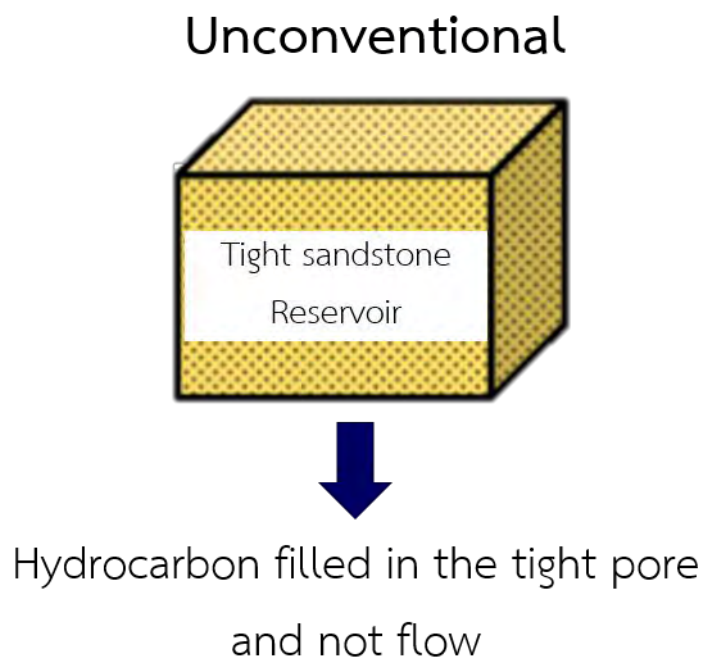


Figure 1.1 Unconventional reservoir fluid flow.

Worldwide Hydrocarbon Resources (BBOE)

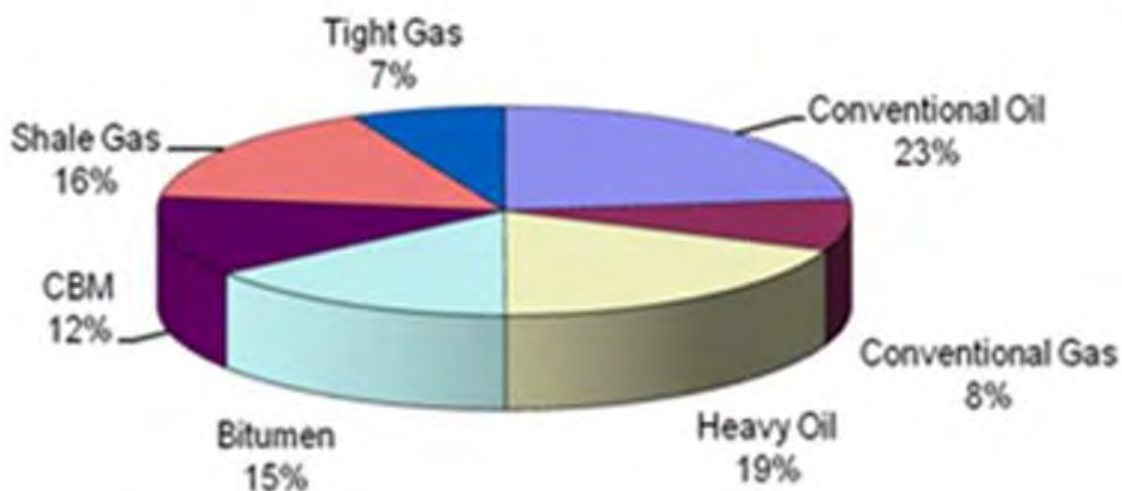


Figure 1.2 Worldwide hydrocarbon resources. Note conventional resources make up less than a third of the total

1.3.2 Tight sandstone

Thirty percent (558 Bcm, 54 Bcfd) of APEC's gas production is from unconventional gas (Figure 1.3). In the North America, Tight gas has a production about 239 and 36 Bcm from China are the worldwide leader of unconventional tight gas production. The U.S has a 6,010 Bcm of proved The Coalbed methane from the unconventional reservoir provides 6 Bcm and have an increase production rate in Australia, Indonesia and Russia. The tight gas play in Mexico (Burgos Basin) and China (Ordos and Sichuan basins) (Figure 1.4) boosts the production of the tight gas resources.

Table EX-6: APEC's Natural Gas Production (2011)

	Bcm/Yr	Bcfd
Conventional	1,270	123
Unconventional	560	54
• Tight Gas	277	27
• Shale Gas	217	21
• CBM	66	6
Total	1,830	177

Figure 1.3 APEC's natural gas production (2011)

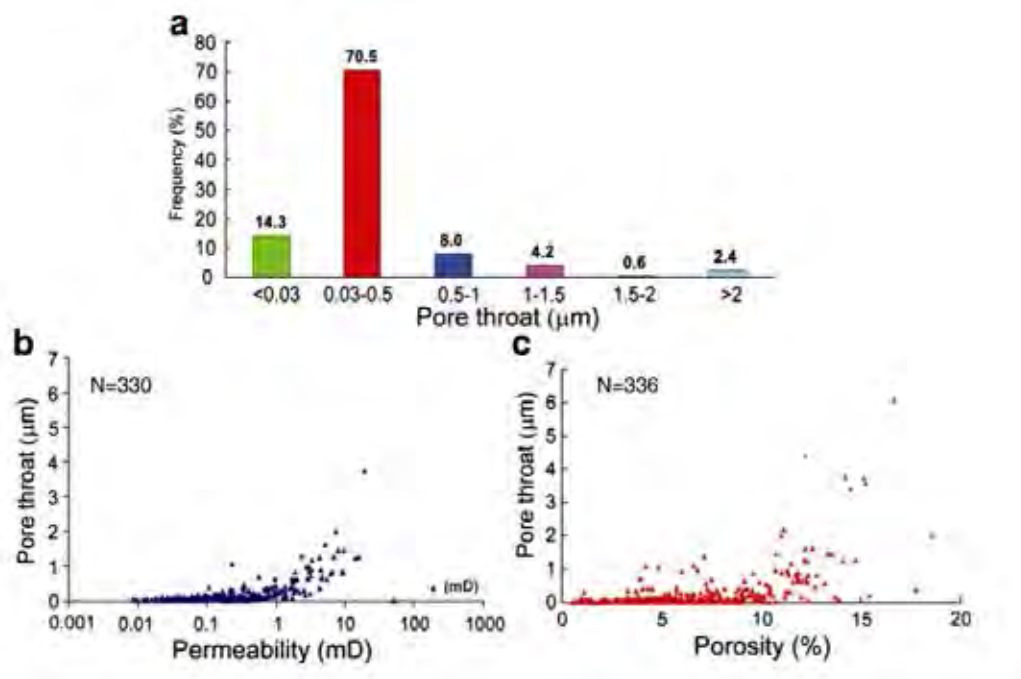


Figure 1.4 EIA assessments of shales gas and tight oil resources in Sichuan Basin, China (EIA,2016)

Tight reservoirs have estimated standard permeabilities of 0.1 md or less are officially recognized by the U.S. Federal Energy Regulatory Commission (AAPG Wiki). This value is the standard for classify a tight reservoir was used to identify widely during the late 1970s and early 1980s to qualify for federally allowed enhanced prices of tight gas. Tight gas reservoir is classified as a low permeability rock in which special well completion techniques are required to stimulate production such as hydraulic fracturing. Thus, most low permeability gas reservoirs are considered “unconventional.”

Tight gas sandstone reservoirs are reservoirs with porosity less than 10%, in situ permeability of less than 1 mD, pore throat diameter less than 1 μm and gas saturation less than 60% (Figure 1.5) (Zou et al. (2010). Tight sandstone reservoir generally hardly to produce to commercial quantity. However, in many countries tight gas sandstone reservoirs are often defined

according to the gas flow (rates) at well site rather than through the permeability cutoff values (Schmoker et al., 1997). It has thus been suggested that tight gas sandstone reservoirs may be best defined from both the petrophysical and economic viewpoints.



. **Figure 1.5** The relationship between pore throat, porosity and permeability in Xujia Formation, China (Zou et al., 2010)

1.3.3 Pore Throat

Pore throat is an intergranular rock, the small pore space at the point where two grains meet (Figure 1.5), which connects two larger pore volumes. The number, size and distribution of the pore throats control many of the resistivity, flow and capillary-pressure characteristics of the rock (Schlumberger Oilfield Glossary, 2015). Although the large pores, the fluid cannot be flow if the pore have no connectivity. Connectivity in the rock can increase by the increasing of the size of pore throats and with increasing number of pore throats which connected the single pore. Pore shape, pore throat size, and pore throat abundance affect the flow dynamics of a reservoir.

Pore-throat sizes in siliceous clastic rocks have a varying size from the millimeter scale to the nanometer scale. The estimated value of the pore and pore-throat sizes range from about 2 to 0.03 mm in tight-gas sandstones (Fig 1.7). The pore-throat size provides a useful perspective

for considering the emplacement of petroleum in consolidated siliciclastic and fluid flow through fine-grained source rocks now being exploited as reservoirs (Nelson, 2009).

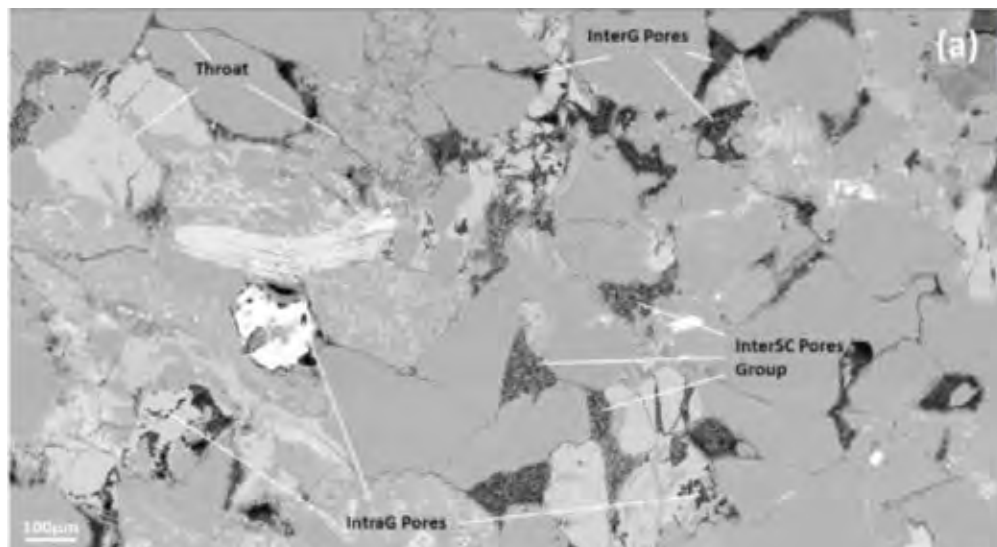


Figure 1.6 Pore throat is the small pore space at the point where two grains meet (Zhenpeng 2015)

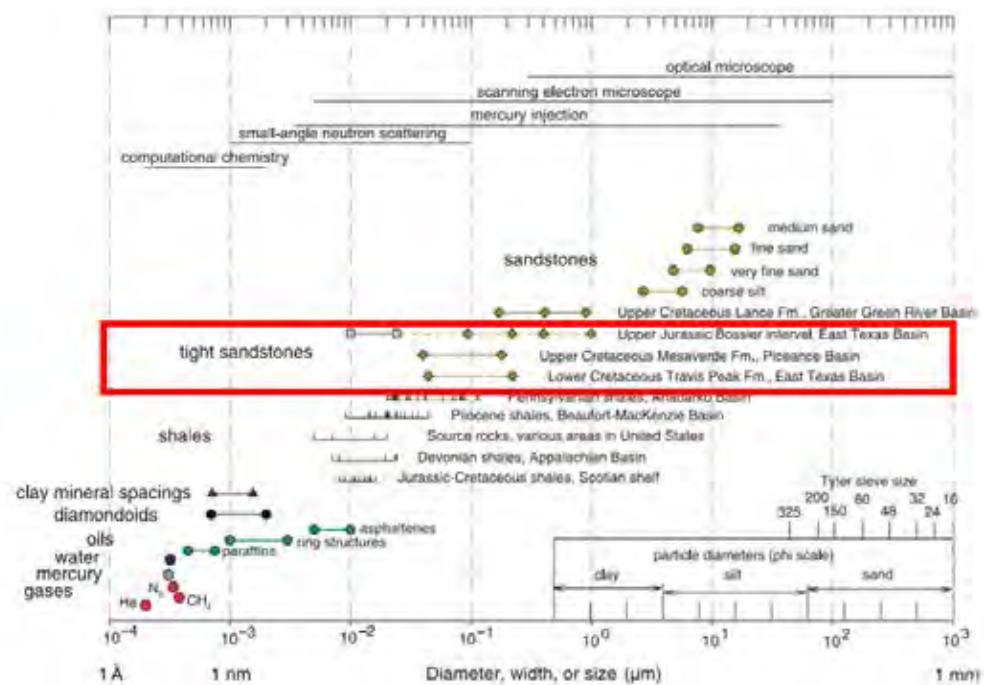


Fig 1.7 Sizes of molecules and pore throats in siliciclastic rocks (Nelson, 2009)

1.3.4 Micro-CT analysis

Micro-CT are used for identifying micropores and the quantity and the connectivity of pores and throats are obtained by reconstruction for the pore scale network. Table 1.1 is a comprehensive description for four analysis methods applied, including the scanning sample size the resolution and the main information for each one (Zhenpeng et al., 2015)

In the CT imaging process, a selected tomography is irradiated by X-ray beam from different directions. After measuring the amount of X-ray penetrating from all directions, the attenuation coefficient of each volume unit can be obtained by solving the multivariate linear equation group. And the CT image of the selected tomography is generated in the computer based on the attenuation coefficient information. The energy of X-ray beam generated from X-ray tube in Micro-CT machine is relatively low, so the small tomography can be scanned clearly (Zhenpeng, 2015). In the CT image, the grayscale represents the X-ray absorption distribution within the object, and local attenuation depends on the chemical composition of the material and its mass density. So it allows the non-destructive examination of the internal properties of the examined sample, which include microarchitecture and morphology of pore space (Zhen peng et al., 2015)

Method	Cores sample size	Resolution	Information
Macro-CT	1-inch plunger	0.62 mm	Porosity histogram and connectivity
Micro-CT	2 mm plunger	1.08 μm	Quantity of pores and throats
Nano-CT	65 μm plunger	65 nm	Quantity of pores and throats

Table 1.1 Test Description for pore structure characterization (Zhenpeng et al., 2015)

Chapter II

Study Area

2.1 Phitsanulok Basin

Phitsanulok Basin or Sirikit Field is in Phitsanulok province, northern of Thailand (Figure 2.1). Phitsanulok Basin is the biggest onshore oil field in Thailand, with STOIP (stock tank oil-initially-in-place) estimated 800 MMB (Bal et al., 1992). Phitsanulok Basin located about 400 km north of Bangkok. The covered area extends about 6000 km². Phitsanulok basin is intracratonic rift basin that formed in Oligocene and Early Miocene by east-west extensional movement. Faults generation in this area forms the appropriate condition for the deposition of the potential source rocks, reservoir rocks, and the trapping systems in this area (C&C reservoirs, 2009). The depositional environments are varying from lacustrine to fluvial depositional environment. The elements of the petroleum system in this area are complete and the main product of the field is principally light oil with 40° API (C&C reservoirs, 2009).



Figure 2.1 Location map of the Sirikit Field, Phitsanulok Basin, Thailand (C&C reservoirs, 2009)

2.2 Regional Tectonic setting and Basin Evolution

Phitsanulok basin was formed in the intracratonic extensional and transtensional basins that originated from the Tertiary Himalayan Orogeny. This controls not only the north-south trending but also basin fills, structural styles, and hydrocarbon habitats of the basin in Thailand (Bal et al, 1992). Figure 2.2 shows a tectonic setting in Thailand. The collision between Indian Plate and Eurasian Plate affect the rotation of Shan-Thai plate relative to Indosinian plate. The strike-slip faults in this area were developed along the paleosuture of Shan-Thai and Indosinian Plate (Kreeprasertkul, 2009).

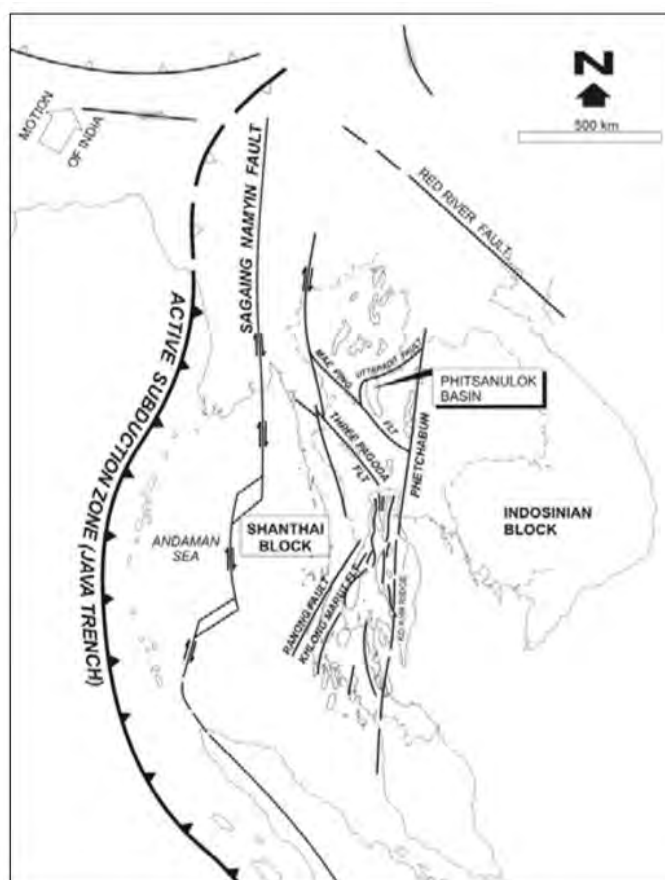


Figure 2.2 Regional Tectonic setting of Thailand. (After Thai Shell Exploration and Production, 1988)

The Structural Evolution of Phitsanulok basin was controlled by 3 principle elements as shown in Figure 2.3, the first element is left lateral Uttaradit Fault System in the north of the

basin which developed the western boundary Fault of Phitsanulok Basin and not extends. The western boundary fault has 8 kilometers estimated depth in the west and shallower to the eastern Flank this affects the irregular shape of Phitsanulok half-graben basin. The next element is Left lateral Mae Ping Fault System located in the southwest of Phitsanulok basin. Finally, right lateral Phetchabun Fault system lying in the east of Phitsanulok basin. The Phitsanulok Basin can be divided into 4 phases by the control of these 3 elements. The first phase begins with extensional tectonics, extensional to transtensional during phase II tectonics, and gradually increasing to transpressional tectonics through phase III and phase IV. (Kreeprasertkul, 2009)

Phase I: Late Oligocene to Early Middle Miocene (Figure 2.3)

The main rifting occurred along the western boundary Fault. The basin rapidly extended in WSW-ENE direction and the small antithetic faults formed in the Eastern Flank. Uttaradit Fault relates to the sinistral strike-slip. The divergence near the junction of movement caused by Mae Ping Fault and Petchabun Fault. Rewarding to the divergence, the convergence regime was developed in the north-east. (Kreeprasertkul, 2009)

Phase II: Early Middle Miocene to Late Middle Miocene (Figure 2.3)

The blockage of Mae Ping Fault and the continued movement of Phetchabun Fault are the main dominant in Phase II. Changing condition has arisen along the western boundary Fault affected to the variation of lacustrine condition to an alluvial condition in Phitsanulok Basin these cause the depositional of Pratu Tao Formation and local unconformity. (Kreeprasertkul, 2009).

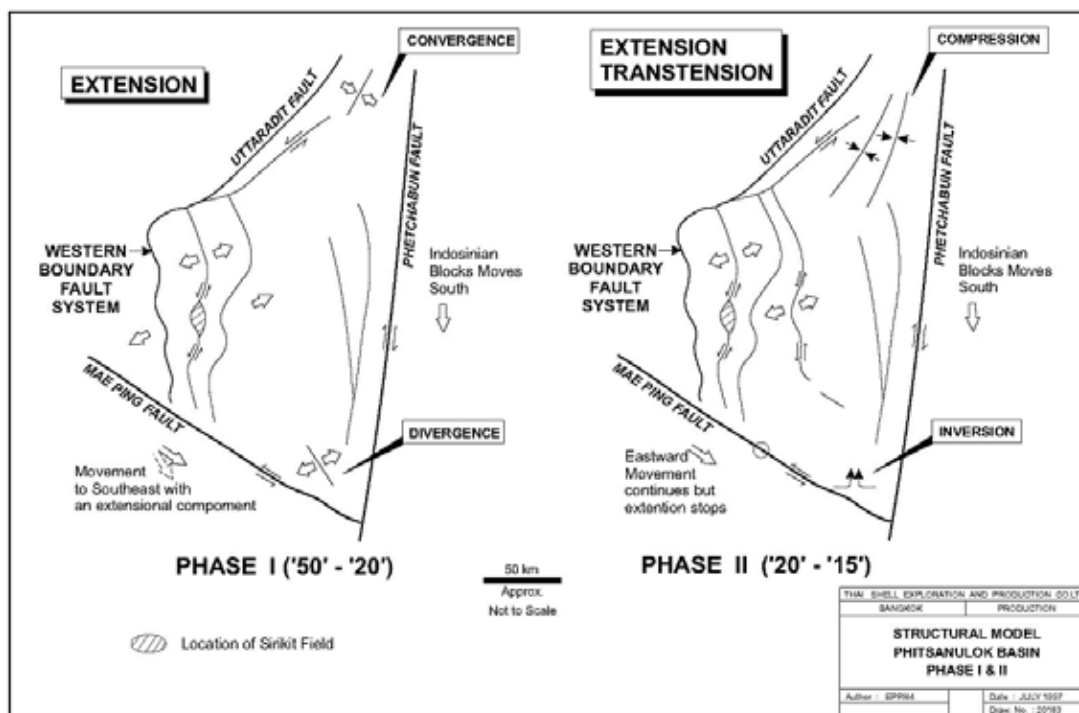


Figure 2.3 Structural model of Phitsanulok Basin (phase I & II) (After Thai Shell Exploration and Production, 1988)

Phase III: Late Middle Miocene (Figure 2.4)

A Hinge zone on the Eastern Flank upthrowing the Nakhon Thai area was introduced by the blockage of Uttaradit and Petchabun Fault. From the discontinue of the extension in the northern part of Phitsanulok Basin; compression continued and overthrusts developed in the Soi Dao area. To the north of Uttaradit Fault, Phichai Graben developed, and Sukhothai Depression possessed the maximum downthrow and the extension continued that result in an anti-clockwise rotation of southern part of Phitsanulok Basin. (Kreepasertkul, 2009).

Phase IV: Late Miocene to recent (Figure 2.4)

Due to the blockage of right lateral Phetchabun Fault, extension discontinued. The compressional stress increased. Inversion feature and dextral wrench fault directly caused the pre-existing structure, paralleled to Phetchabun Fault. Thus, complex Riedel fault pattern developed at Tertiary period. The slow and uniform subsidence took place. In addition, basaltic and rhyolitic volcanism, which is younger, accompanied this phase (Kreepasertkul, 2009).

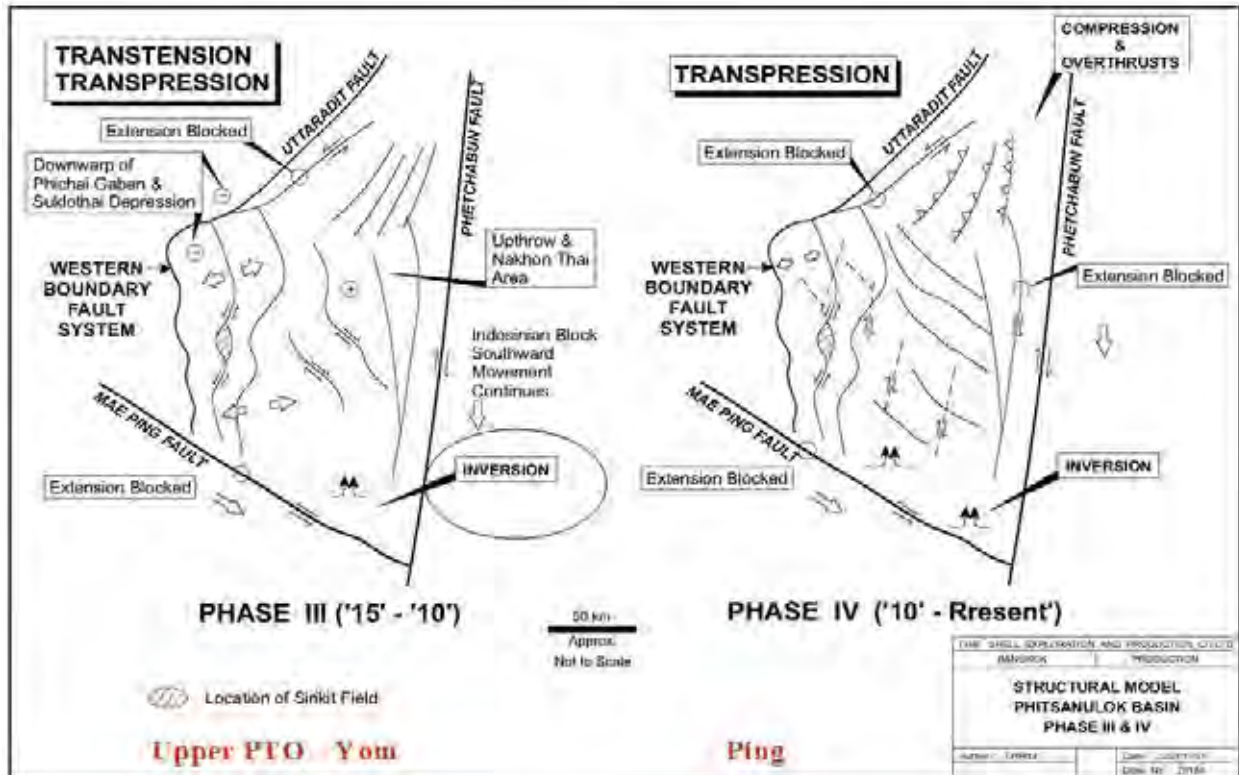


Figure 2.4 Structural model of Phitsanulok Basin (phase III & IV) (After Thai Shell Exploration and Production, 1988)

2.3 Stratigraphy

The stratigraphy of Phitsanulok basin can be divided into 8 lithostratigraphic units from Oligocene to recent as shown in Figure 2.5 and 2.7 (Thai Shell Exploration and Production, 1988). The deposition environment varying from alluvial to lacustrine deposit that related to structural control in this area that shows in Figure 2.6. Three types of basin fill in Phitsanulok Basin defined as alluvial fans and alluvial plain in the lowest part, lacustrine and alluvial plains in the middle part, and alluvial plain and alluvial fans in the upper part (Kreeprasertkul, 2009).

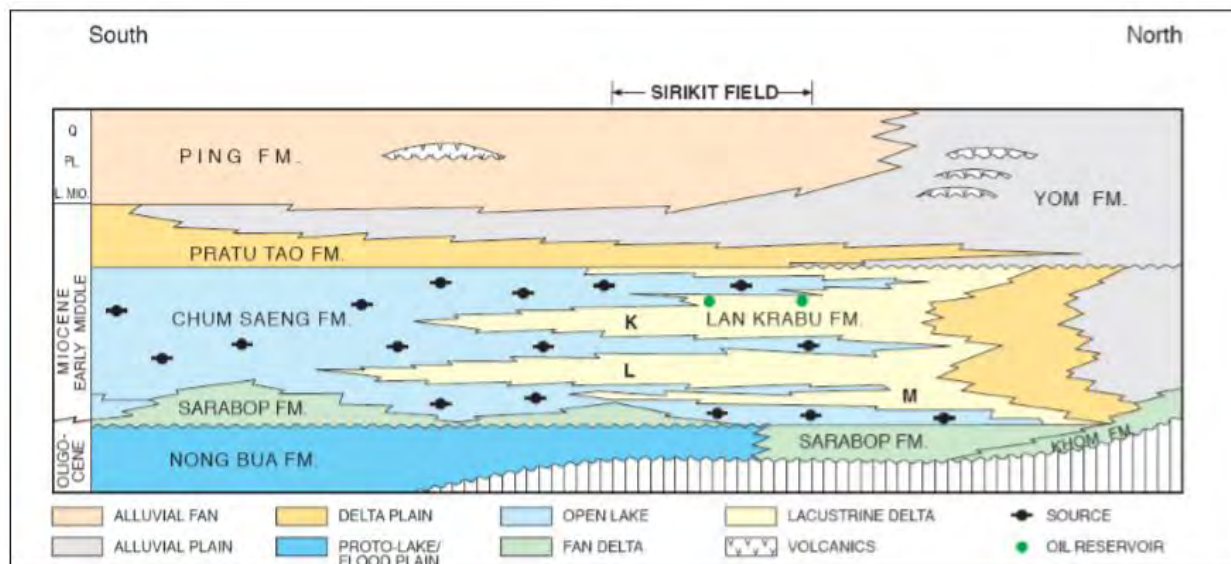


Figure 2.5 Schematic S-N cross section of Sirikit Field shows the Stratigraphy of Phitsanulok Basin. Lithostratigraphy comprises 8 units (After Thai Shell Exploration and Production, 1988)

In the Oligocene, **Nong Bua Formation**, **Khom Formation**, and **Sarabob Formation** abruptly deposit and covered pre-Tertiary units. These related to the high energy deposition environment of the western Boundary Fault escarpment. In Addition, alluvial plain covered the basin axis and this affected the several faults blocks in this area. (Kreepasertkul, 2009).

Late Oligocene time, the subsidence of basin continued that originated the open lacustrine deposit of **Chum Saeng Formation**, which extend an area of 4,000 square kilometers. Chum Saeng Formation is composed of organic-rich claystone. Moreover, the lacustrine transgression varied due to the varying of base level, the rate of subsidence, sedimentation, and climate. In the Mid Early Miocene, lacustrine deltas prograde to the south and predominated in the southern part of the basin (Kreepasertkul, 2009).

The deltaic deposit of **Lan Krabu Formation** consists of sandstone interbedded claystone. At the end of Early Miocene, the open lacustrine deposit re-established in the central of the basin. The organic-rich claystone of Chum Saeng Formation deposited over Lan Krabu Formation

The fluvio-delta deposit is predominant. The delta plain and alluvial plain of **Pratu Tao Formation** and **Yom Formation** developed during Middle Miocene. Pratu Tao Formation contains the floodplain shale and Yom Formation consist of Sandy shale. The transtensional in this time changed into the transpressional that result in the change of depositional environment into the

meandering fluvial system of Yom Formation and to alluvial fans of Ping Formation which consist of sand and gravel.

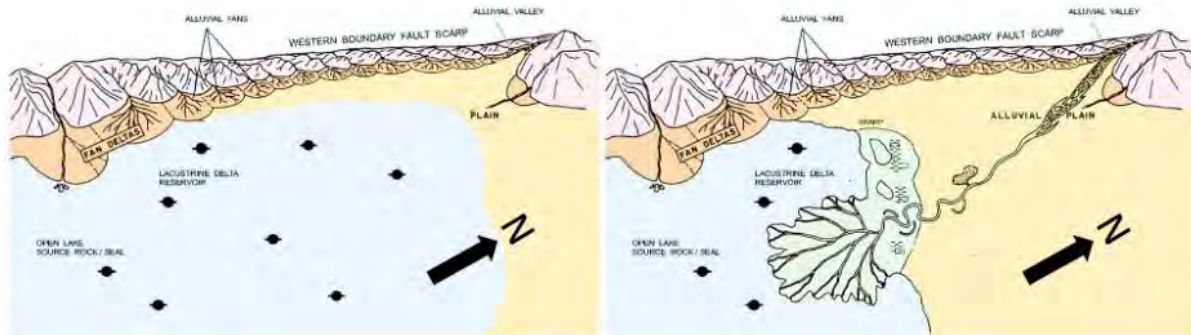


Figure 2.6 Schematic depositional environment of Phitsanulok Basin. (After Thai Shell Exploration and Production, 1988)

AGE	FORMATION	THICKNESS (UP TO)	LITHOLOGY	DESCRIPTION	ENVIRONMENT
LATE MIOCENE - RECENT	PING	1,300 m	SANDS/GRAVELS WITH ASSOCIATED CLAYS	Sands, clear, white, coarse grained, occasionally gravel. Gravels, variegated, lithic. Clays, varicoloured, sandy, silty	Alluvial fans
MIDDLE MIOCENE - LATE MIOCENE	YOM	1,000 m	SANDS/CLAYS	Sands, clear, white, coarse grained, occasionally gravel. Clays, varicoloured, sandy, silty	Alluvial plain
	PRATU TAO	1,400 m	SAND (STONES)/CLAY (STONES)	Sand (stones), clear, white, fine-coarse grained. Clay (stones), reddish brown, varicoloured, sandy, silty	Fluvial
EARLY MIOCENE - MIDDLE MIOCENE	LAN KRABU - CHUM SAENG	2,200 m	CLAYSTONES AND SILTSTONES/SANDSTONES	Claystones and siltstones, grey, silty, occasionally gastropod-bearing and carbonaceous. Sandstones, clear, white, grey, fine-medium grained, thinly bedded	Fluvio-delta & Lacustrine
OLIGOCENE - EARLY MIOCENE	SARABOP - NONG BUA	1,200 m	CLAYSTONES	Claystones, reddish brown, occasionally grey to varicoloured, with minor coarse-fine lithic sandstones	Alluvial fans & Alluvial plain
PRE-TERTIARY BASEMENT			MESOZOIC - PALEOZOIC CLASTIC, CARBONATE. VOLCANICLASTIC IGNEOUS, AND METAMORPHIC ROCKS		

Figure 6 Stratigraphy and depositional environment of the Phitsanulok Basin

Figure 2.7 Stratigraphy of the Phitsanulok Basin (C&C reservoirs, 2009)

2.4 Petroleum system

2.4.1 Source rock

Source rocks in the Phitsanulok basin were deposited in three environments

- Open lacustrine environment
- Fluvio lacustrine environment
- Marginal lacustrine swamp

The source rocks are up to 400 m thick and belong to the Lower-Middle Miocene Chum Saeng Formation. Coals are also present in this formation. Freshwater and terrestrial palynofacies and freshwater gastropod fossils are the key to define the lacustrine deposit of the source rock (Figure 2.9) (C&C Reservoirs, 2009). The source rocks have a high content of Type I kerogen derived from freshwater algae with an estimated 2.7 %TOC and Type III kerogen from higher plants (Figure 2.8). By contrast, the fluvio-lacustrine of Lan Krabu Formation consists of type II and III source rocks with lower %TOC (Figure 2.8). Marginal lacustrine swamp contains carbonaceous shale and lignite with estimated 14 %TOC (Figure 2.8) (Bal et al., 1992)

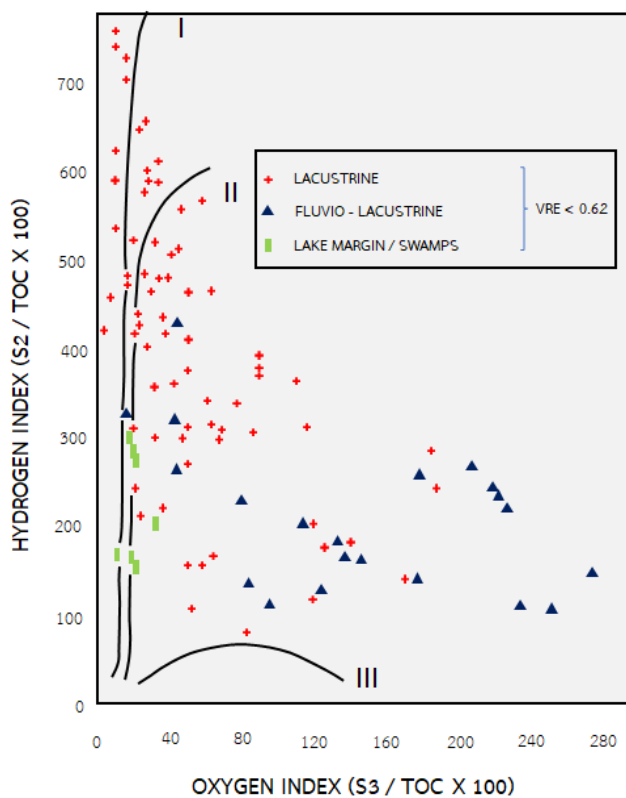


Figure 2.8 HI versus OI plot of source rocks in Phitsanulok Basin. (Illustrated from Bal et al., 1992)

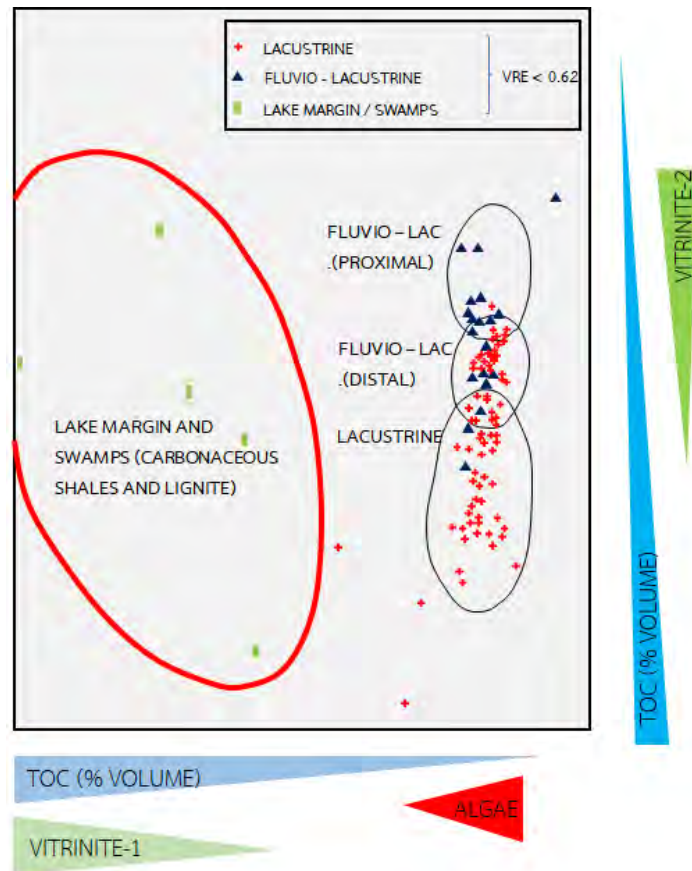


Figure 2.9 Marceral Analysis (Illustrated from Bal et al., 1992)

2.4.2 Reservoir

The predominant reservoirs in Phitsanulok Basin are the reservoirs of Early Miocene deltaic sandstone of Lan Krabu Formation. The reservoir quality and distribution in this formation are various, relate to rapid lateral and vertical facies change. Lan Krabu Formation is consisting of 4 reservoir subunits which can be subdivided as D, K, L, and M units that interfingering with the lacustrine Chum Saeng Formation (C&C Reservoirs, 2009). M Reservoirs in Phitsanulok Basin was defined as Tight reservoir which low productivity and low recovery factor could be due to the reservoir quality and connectivity problems that are expected to be improved by the hydraulic fracturing (Kiatrabile et al., 2016).

2.4.3 Seal

Lan Krabu Formation sealed by claystone of Chum Saeng Formation. This reservoir-seal pair relate to cyclic delta progradation and lacustrine transgression of this area. Pratu Tao and Yom seal potential due to thin and laterally discontinuous intraformational seals which make a trap on this level easily leaked. (Bal et al., 1992) The fault occurrence in this area relates to the potential of clay smear along the fault plane. Clay smear essentially provides the lateral seal for hydrocarbon retention. Particularly, lacustrine claystone of Chum Saeng Formation has good smear potential for Lan Krabu Formation flood plain claystones of Pratu Tao Formation has less smear potential. Lateral seal for the smaller accumulations in the Pratu Tao formation is formed by juxtaposition seal. (Kreeprasertkul, 2009).

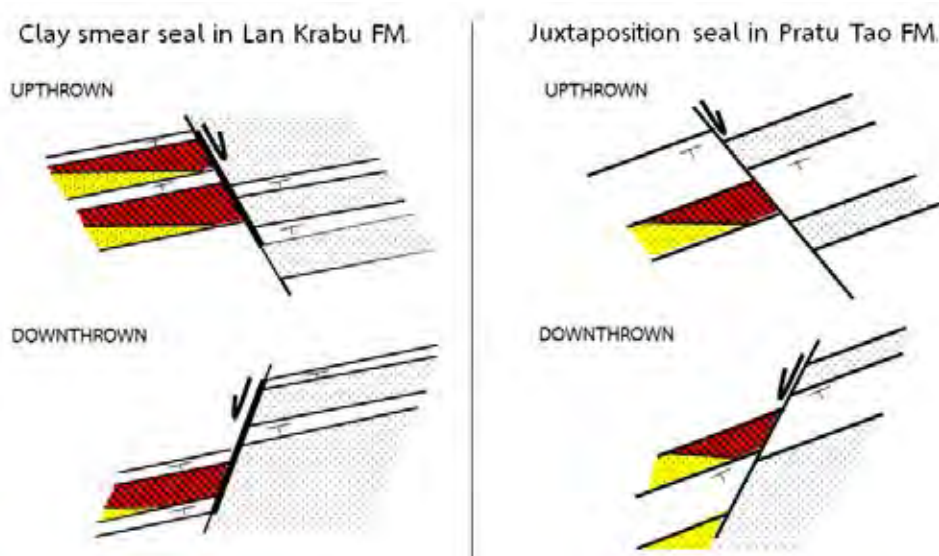


Figure 2.10 Fault sealing and trapping mode in Phitsanulok Basin. (Illustrated from Thai Shell Exploration and Production, 1988)

2.4.4 Trap

The trap in the Phitsanulok basin control by the complex fault patterns. Tilted fault blocks in Phitsanulok are broken into numerous compartments by intense wrench-related faulting. Fault trapping mode in Phitsanulok basin consists of upthrown (Sirikit and Pru Krathiam area), downthrown (Nong Tum area), and combined (Thap Reat area) fault closure. The stratigraphic traps also show in this basin, such as onlap, pinch out, diagenetic trap and

unconformity Due to lateral and vertical facies changes and fault that cut through the formation, it developed fault juxtaposition of reservoirs against interbedded claystone. Fault sealed by clay smear have more potential in trapping a longer column of hydrocarbon (Kreepasertkul,2009).

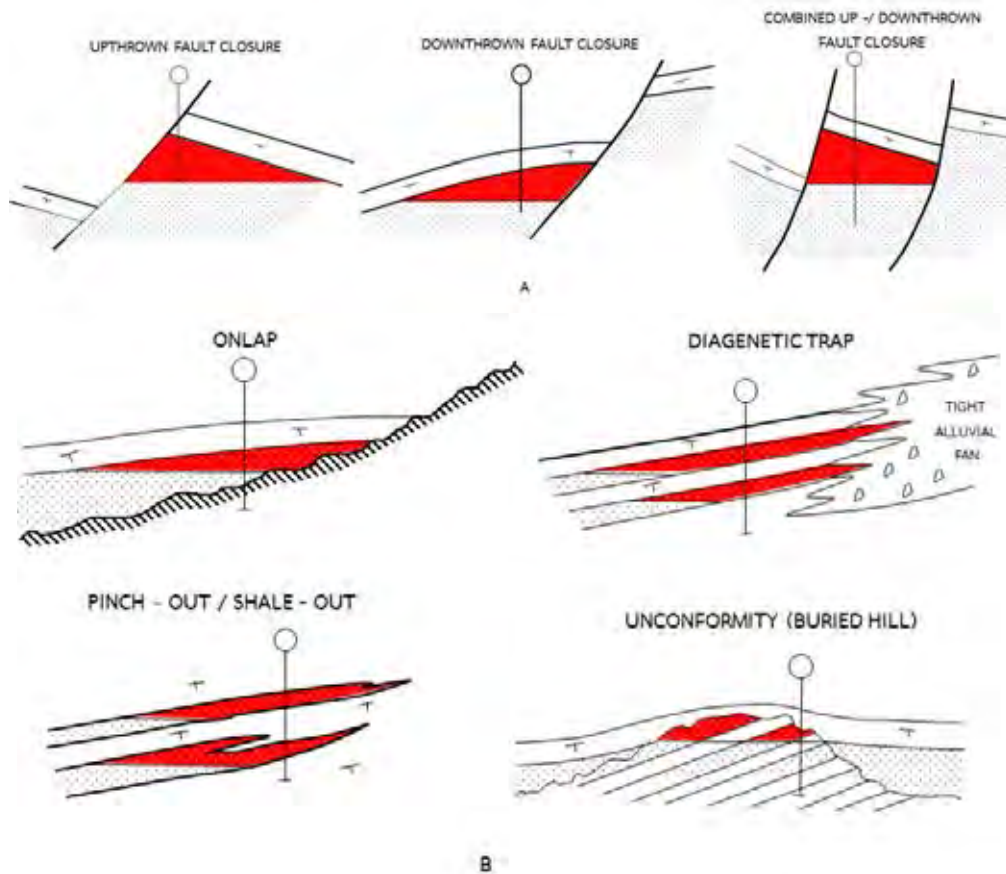


Figure 2.11 Fault sealing and trapping mode in Phitsanulok Basin. (Illustrated from Shell Exploration and Production, 1988)

Chapter III

Methodology

The characterization tight rocks, very tiny and complex, in microscopic in term of pore structure which includes pore type, pore scale, pore origin and pore connectivity, it is difficult to characterize pore structure through conventional testing. Many new methods are developed and applied in the study of tight oil reservoir such as Micro-CT. In the rock physics analysis filed, Micro-CT have been a useful technology which has been widely use in core heterogeneity characterization, porosity measurement, saturation measurement, and flow experiment study

3.1 Samples preparation

Three samples of tight sandstone were selected for this study. The three samples are tight sandstone in Phitsanulok Basin from the same borehole. Most of the samples were cut into small prisms size 0.5 mm x 0.5 mm x 5 mm then the prisms were glued on a glass slide and polished into small cylinders which 0.5 mm diameter x 5 mm length.

3.2 Synchrotron X-ray Tomography

Synchrotron experimental set up is shown in Figure 3.1 The X- ray beam is the source from Synchrotron and run through monochromator with a monochromatic X-ray energy of 18 keV. The incident X- ray strike the sample surface on a rotational stage in a long axis vertical arrangement. The sample was rotated 0.125 per X-ray beam shot for a total of 180. The transmitted X-ray beam was converted to a visible wavelength by scintillator. After that the visible light projected on a CCD detector that be a 2D data which was used to reconstruct a 3D image (Kanitpanyacharoen et al., 2012)

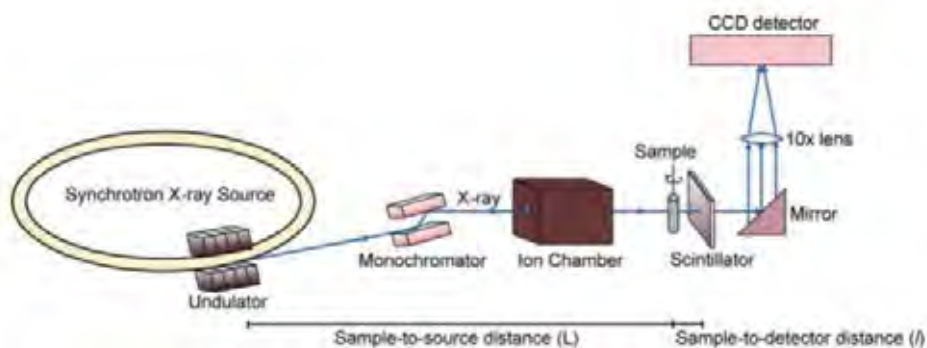


Figure 3.1 Schematic diagram of the Synchrotron X-ray Micro-CT experiment. (Kanitpanyacharoen et al., 2013)

Materials have a different X-ray absorption ability according to Beer Lambert 's law (Figure 3.2) The different absorption coefficient depends on atomic number and density of the elements that represent in 32-bit TIF in a wide range of grayscale values (256 shades) (Kanitpanyacharoen et al., 2012).

The X-ray attenuation or linear Attenuation Coefficient (LAC), as defined by Wellington and Vinegar (1987) is a measure of the transmissivity or absorptivity of a sample to the incident X-rays and is largely a function of both electron density, e , and effective atomic number, Z_e . LAC depend on the incident photon energy from a synchrotron X-ray beam, E . High atomic number in mineral will be shown in bright tone and low atomic number will be shown in dark grayscale also as a pore.

Avizo software was used to identify the structure inside the rock by using the different grayscale. The software can calculate the quantity of pore and porosity also can simulate a fluid flow simulation in 3D configuration.

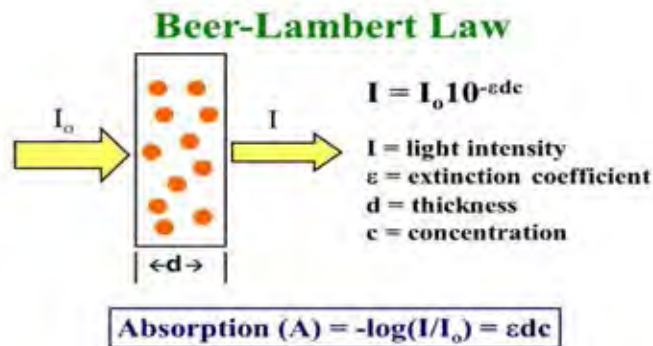


Figure 3.2 Beer-Lambert Law show that the light intensity come into the material has a different value with the light intensity throughout. (www.slideplayer.com)

3.2 Data Analysis

Avizo Fire was used to perform the image segmentation on the tight sandstone sample and to create a representation of the pore space surface. Some area of the core images contained artifacts such as beam-hardening rings or concentric ring and were disinterested for model study. Images data had to be cropped significantly into a voxel size(μm) to be use in simulation. The

thresholding segmentation was identified through the Label Analysis Avizo module. Grey scale values for the pore space and minerals were investigated by Glemser (2008). The grey scale value from 0–85 thresholding scale represented pore-space while 86–255 represented rock matrix. An example of a grey-scale image pore space extracted by thresholding (Blue) is shown in Figure 3.4 and before segmentation in Figure 3.3. After the segmentation the Avizo program can illustrated the single pore simulation in the sample (Figure 3.5)

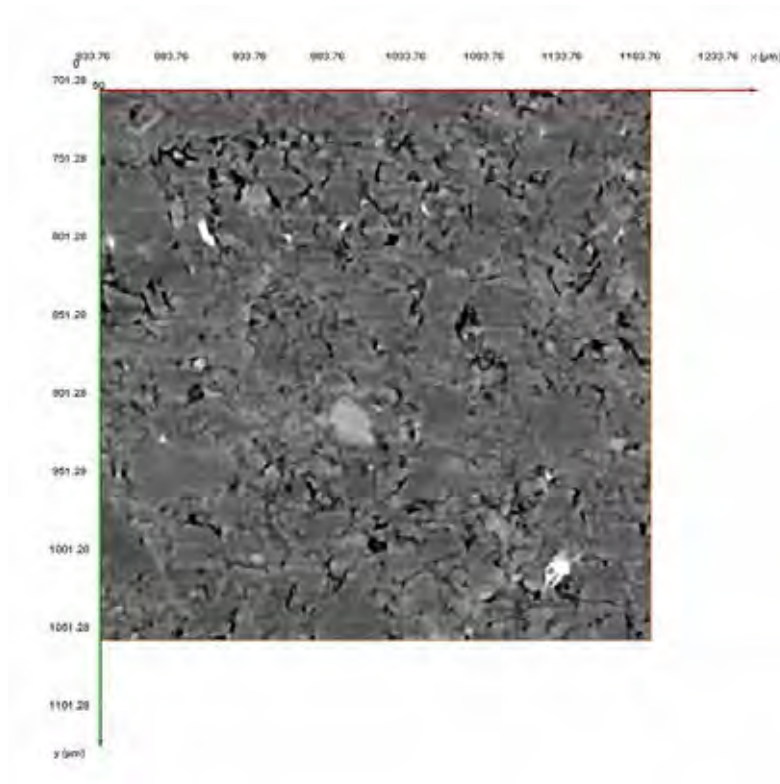


Figure 3.3 Image before thresholding segmentation

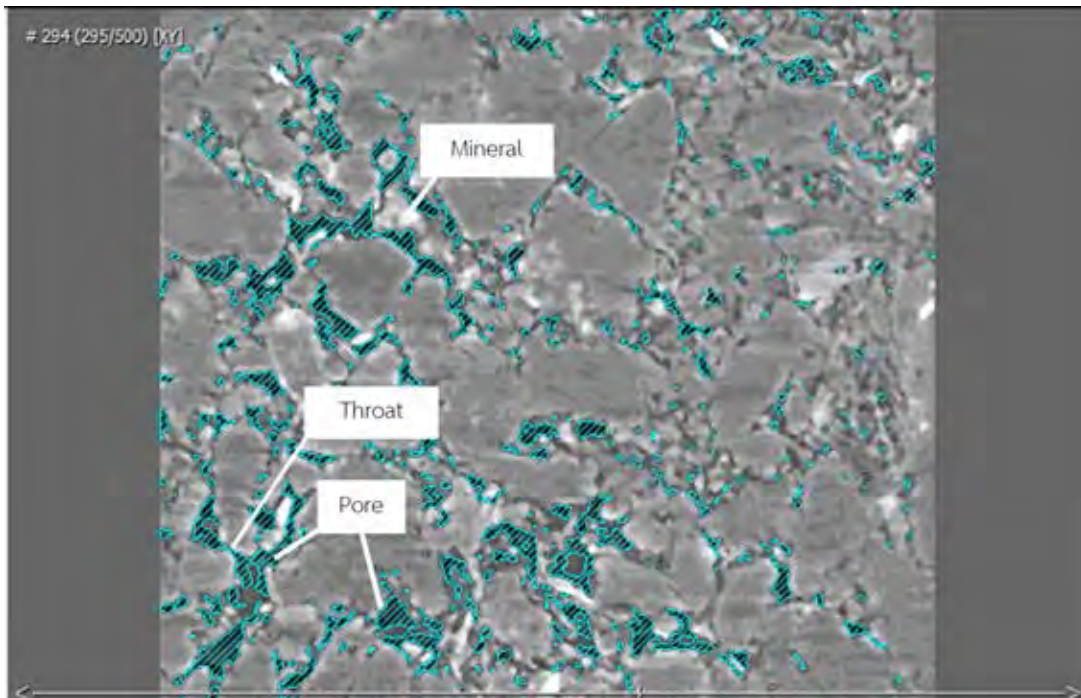


Figure 3.4 Different shades of grayscale was used to identify the material

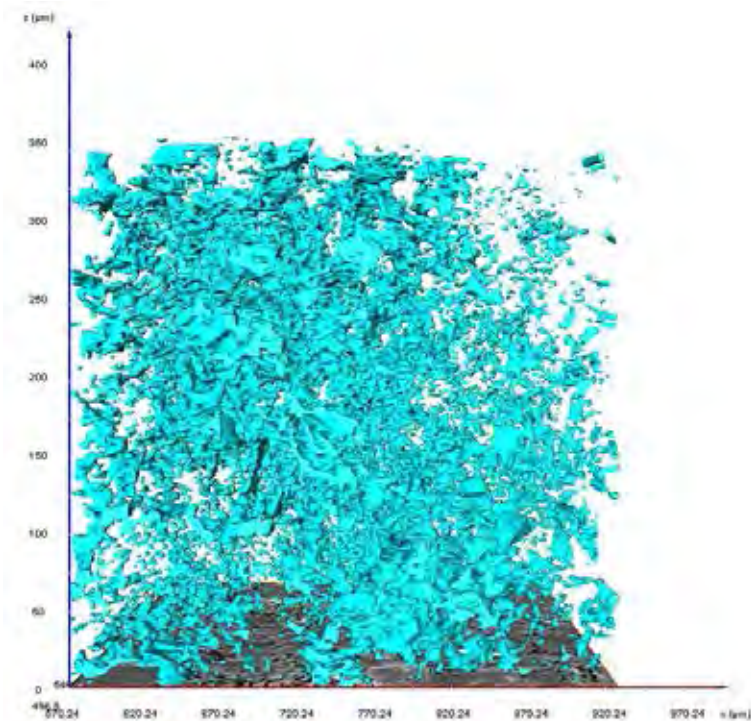


Figure 3.5 Illustration of the selected single pore

The absolute permeability is the parameter used to characterize pore which allows of a single-phase fluid flow. The effective porosity and quantity of throat can provide a flow channel for the fluid. In Avizo, flow simulation was realized by use of a single-phase laminar flow and the absolute permeability derived from the of Darcy's law. The 3D simulation which is the results from permeability are illustrated (Figure 3.6).

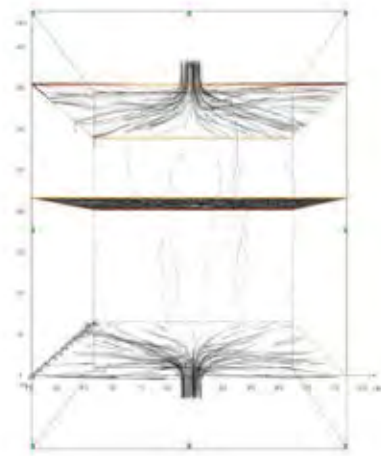


Figure 3.6 Flow simulation which is the results from permeability

To study pore throat it necessary to study the pore diameter and orientation that was divided into four step module the first step is pore detection which the result image will show in the thresholding binary image where one of the intensity level equal to pore and one equal to the matrix (Figure 3.7). Next is Pore post-processing, the small objects are removed in this step. The objects boundaries are smooth, and some objects are disconnected. The third is to custom measure group definition to determine the distribution of pore diameter. The Avizo label analysis module allows computation of a set of measure for each particle of a 3D image once the individual analysis has performed a histogram (Figure 3.8) of a given measure was be plotted in order to produce a representation of the measure distribution. The EqDiameter was used in this step (Equation 1). Finally, customization of measure definition to compute the sphericity of pore and throat.



Figure 3.7 The binary image where one of the intensity levels equal to pore and one equal to the matrix in pore detection

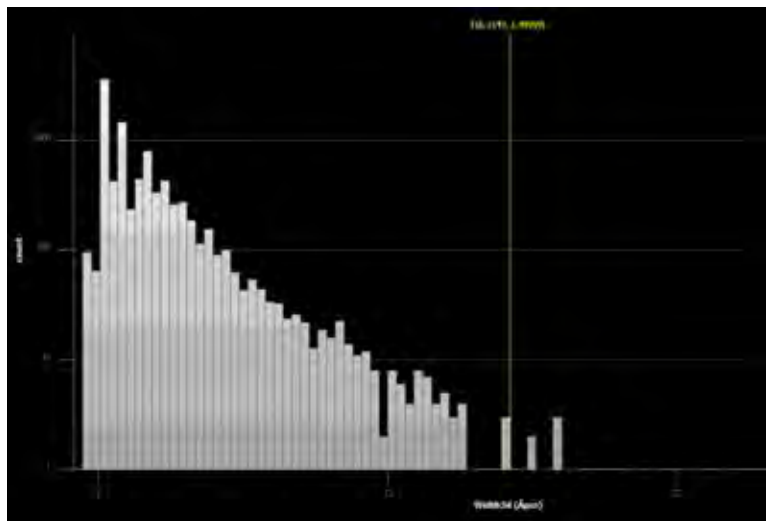


Figure 3.8 The analysis diameter histogram

EqDiameter=36 Volume3d

(1)

To determine how the pore were connected. Pore were connected if they shared a common face while pore voxels that shared only common edges or points were not considered connected. The “Connected Components” module in Avizo was used to find connected pore. Auto skeleton module will use to model the connectivity between pore chamber and illustrate into 3D skeleton which will be identify as pore throat (Figure 3.9)

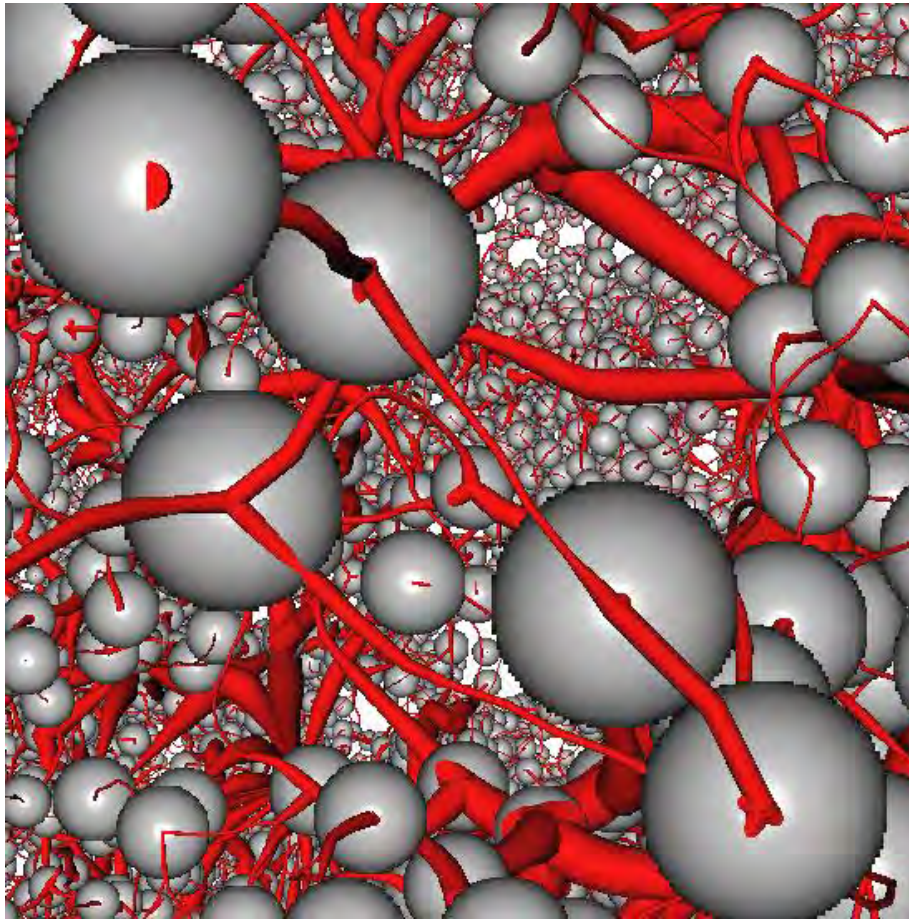


Figure 3.9 3D Simulation of Auto skeleton module

Chapter IV

Results

In Synchrotron X-ray Tomography, three samples of tight sandstone were selected for this study (PH1, PH2, and PH3). Most of the samples were cut into small prisms size 0.5 mm x 0.5 mm x 5 mm then the prisms were glued on a glass slide and polished into small cylinders which 0.5 mm diameter x 5 mm length.

Avizo Fire was used to perform the image segmentation on the tight sandstone sample and to create a representation of the pore space surface. Images data had to be cropped significantly into a 500x500x500 voxel size (0.72 μm) to be use in simulation. Each sample was randomly selected into 3 VOI, finally the 9 VOI are shown in Figure 4.1. The thresholding segmentation was identified through the Label Analysis Avizo module. Grey scale values for the pore space and minerals were investigated by Glemser (2008). The grey scale value from 0–65 thresholding scale represented pore-space (Figure 4.2a) while 65–255 represented rock matrix (Figure 4.2b)

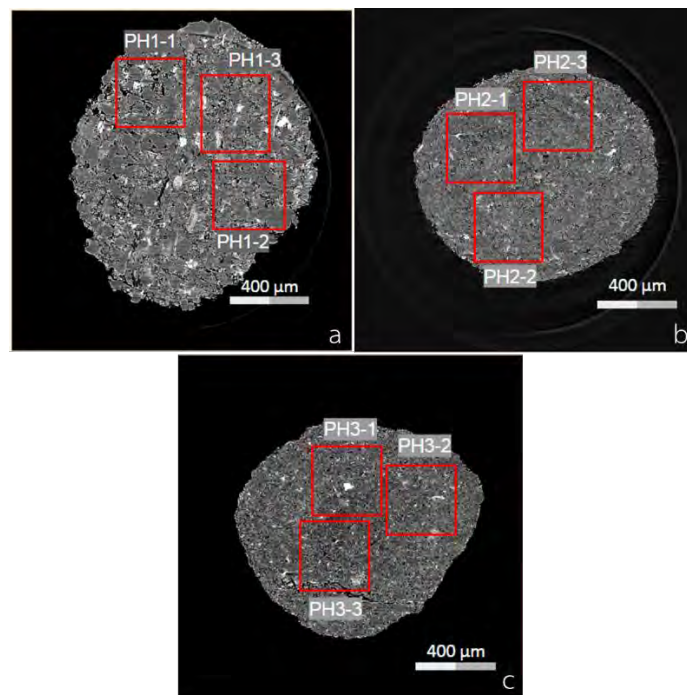


Figure 4.1 Three sample of tight sandstone was divided into 3 area (Total 9 VOI) Sample PH1, PH2, and PH3 are a, b, and c respectively

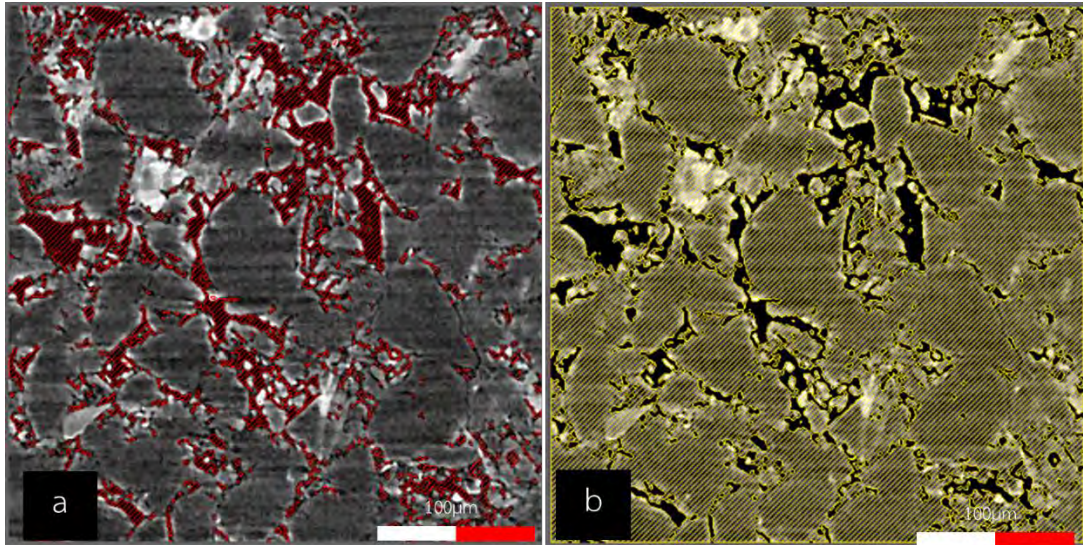


Figure 4.2 (a) The grey scale value from 0–65 thresholding scale represented pore-space while **(b)** 65–255 thresholding scale represented rock matrix

4.1 Grain Size Analysis

Grain size analysis of each VOI are classified to diameter of grain size via Wenworth scale (Figure 4.3) Grain size analysis method of the samples was analyzed by Label analysis module. The results show that the grain size of three samples are varying from 3.9 to 125 micrometers which are very fine silt to very fine sand size due to the Wenworth scale. Figure 4.4 show that PH1 sample have the biggest grain size from three samples. Grain size class in this sample are varying from very fine silt to very fine sand which the greatest number of grains is coarse silt. The average of grain size in PH1 is 61.15 μm which is classified into very fine sand class. Grain in PH1 sample shows well sorted of grains.

For PH2, grain size class are from very fine silt to coarse silt the greatest number of grains is in medium size and the second is fine silt. The average of grain size diameter is 30.01 μm which is classified into medium silt size of grain and shows very well sorted of grain inside the sample. PH3 sample dominated with the grain size like PH2 which the greatest grain is in medium silt class but the second is coarse silt class. Range of grain size in PH3 are varying from fine silt to coarse silt which the average diameter is 41.11 μm that is classified into coarse silt size. In this sample shows very well sorted of grain.

Millimeters (mm)	Micrometers (μm)	Phi (φ)	Wentworth size class	
4096		-12.0	Boulder	
256		-8.0	Cobble	
64		-6.0	Pebble	
4		-2.0	Granule	
2.00		-1.0	Sand	
1.00		0.0		Very coarse sand
1/2	500	1.0		Coarse sand
1/4	250	2.0		Medium sand
1/8	125	3.0		Fine sand
1/16	63	4.0	Very fine sand	
1/32	31	5.0	Silt	
1/64	15.6	6.0		Coarse silt
1/128	7.8	7.0		Medium silt
1/256	3.9	8.0		Fine silt
0.00006	0.06	14.0	Mud	

Figure 4.3 Grain size classification which analyzed due to grain diameter (Wentworth, 1922)

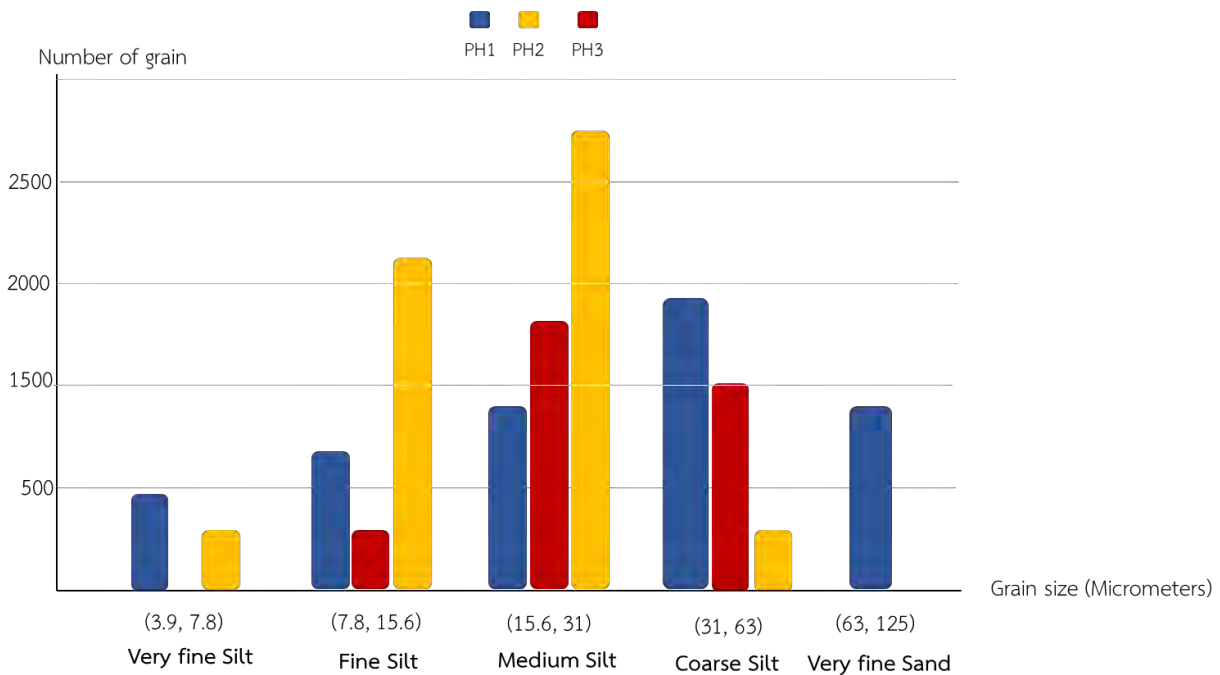


Figure 4. 4 Grain size analysis classified by grain diameter based on Wentworth scale

4.2 Pore Classification

Synchrotron X-ray Tomography can use in primary identification of pore shape. In this study use pore shape classification based on pore shape of reservoir rock which classified by Louck et al. (2012) In Figure 4.5 show that pores are classified in to main three types (Mineral Matrix Pores, Organic-Matter Pores, Fracture Pores). For this study, Mineral Matrix Pores (Interparticle Pores) and Fracture Pores are the major of pores which generally found in three sample.

Two classes of pore in interparticle pores type which show in three sample are pores between grains and Pores at the edge of rigid grains. Pore between grains (Figure 4.6a) are the space around each grain in rock matrix or space between pore. This pore type found normally in all sample in this study but dominated in the PH1 sample. Pore between grains usually forms in low to medium compaction rate of rocks and can enhance the porosity and permeability in the rock in the normal rock reservoir.

For pore at the edge of rigid grains (Figure 4.6b) is the small space at the edge of the grain which usually found in high compaction of rock or very small grain size. This pore type can be found in the whole rock samples in this study but dominate in PH2 and PH3 sample. This pore type can enhance the porosity but in the other hand some situation the permeability in rocks will lower than the other pore type.

Fracture pores (Figure 4.6c), this pore type is the widest space of pore type in rock samples. Fracture pore can find in only PH3 sample. This pore type well enhances porosity and permeability in the rock that have very small grain size and high compaction.













A		Organic-Matter Pores	Fracture Pores
Mineral Matrix Pores Pores between or within mineral particles		Pores within organic matter	Pores not controlled by individual particles
Interparticle Pores	Intraparticle Pores	Organic-Matter Pores	Fracture Pores
 Pores between grains	 Intercrystalline pores within pyrite framboids		
 Pores between crystals	 Pores within peloids or pellets		
 Pores between clay platelets	 Dissolution-rim pores		
 Pores at the edge of rigid grains	 Pores within fossil bodies		
	 Moldic pores after a crystal		
	 Moldic pores after a fossil		

Figure 4.5 Pore shape classification (Louck et al.,2012)

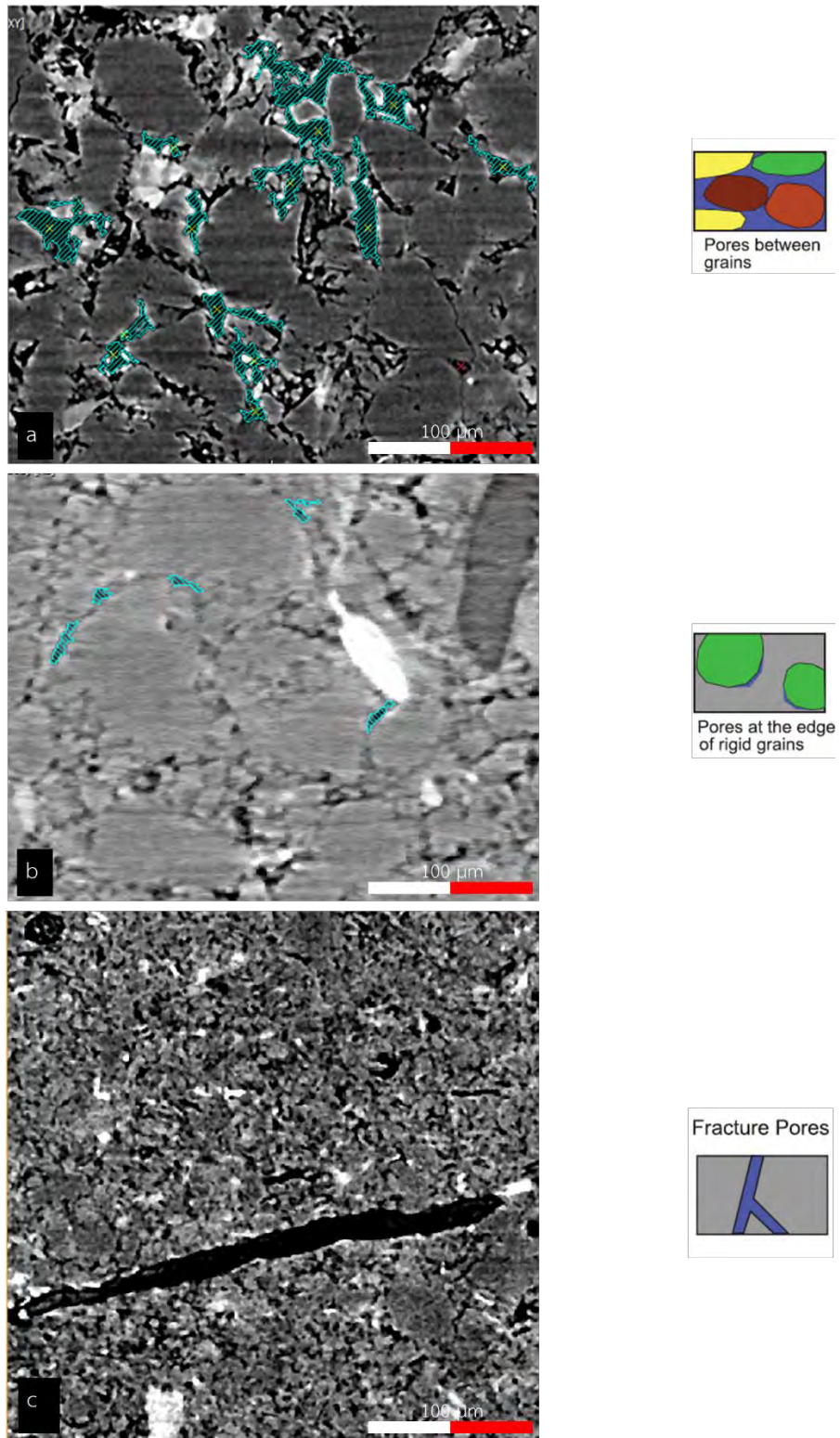


Figure 4.6 Three pores type f in samples of this study (a) Pores between grains (b) Pores at the edge of rigid grains (c) Fracture pores

4.3 3D Pore shape and Volume

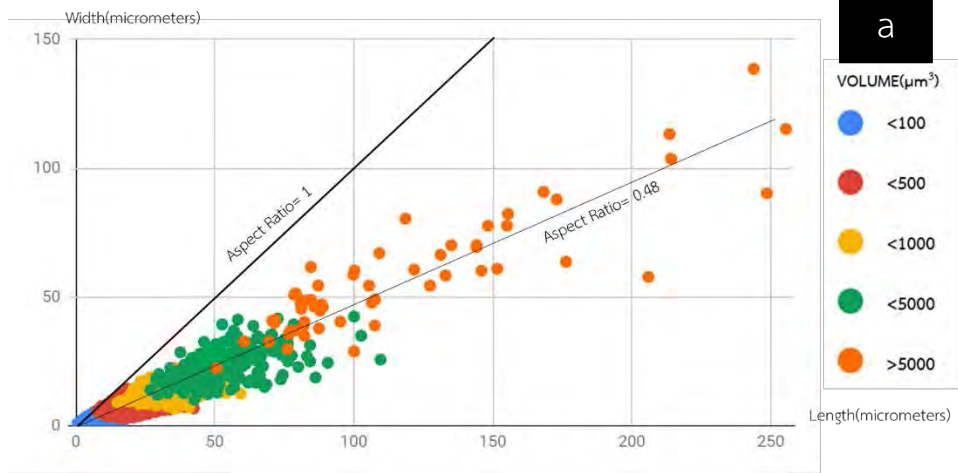
To study of pore shape character in rock sample the Label analysis module in Avizo software are used. The module will calculation width, length, radius, and volume in micrometers scale of selected area. Pore shape identification uses width versus length of the object to identify the character of pore in the samples. If aspect ratio of width and length is 1 pore will consider to be sphere.

PH1 sample show the plot between width and length in Figure 4.7a. Average aspect ratio of PH1 is 0.48. This value of aspect ratio shows that pore in PH1 have shape like oval. The data of PH1 show trend of data in linear. The volume of most pore in PH1 is in the range of 1000 to 5000 μm^3 . In the volume more than 5000 μm^3 have high different between each value so it shows the wide spread of data in this volume of PH1.

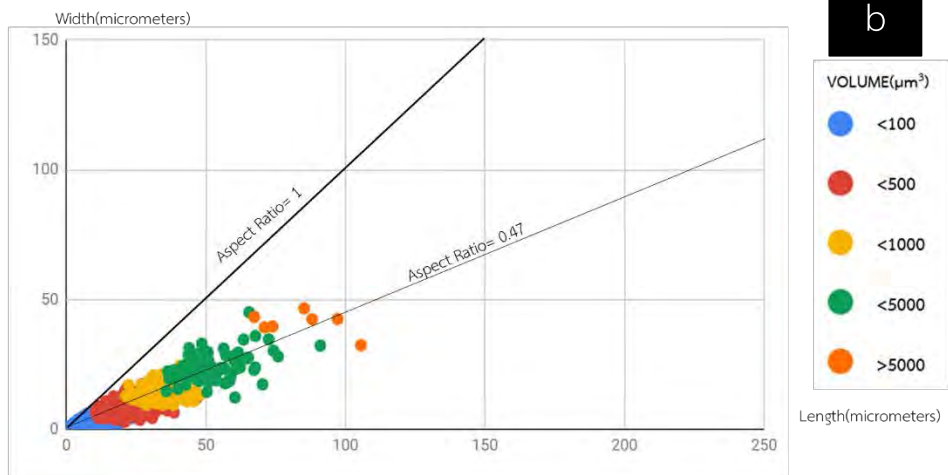
In figure 4.7b shows width versus length plot of PH2 sample. This sample have 0.47 value of an average aspect ratio which approximate to aspect ratio in PH1. But the volume of pore which more than 5000 μm^3 is lower than PH1. In the same as value of volume in range of 1000 to 5000 μm^3 have count number lower than PH1. This will affect to the porosity in PH2 that possible to lower than PH1 too. The low volume of PH1 pore space it may be affect from the pore shape that have a greatest number of pores at the edge of rigid grains.

For PH3 sample, this sample have an average aspect ratio lowest from the others. The average aspect ratio is 0.37 and shown the linear trend of data. This can be considered that the pore shape of PH3 is flatter or more tabular than others. The volume of pore in PH3 are mostly in range from 500 to 1000 μm^3 . The second number of ranges is 1000 to 4000 μm^3 . This may affect from the greatest count number of pores at the edge of rigid grain. By the way, PH3 have a like horizontal linear data in range of >5000 μm^3 . Aspect ratio of this range shows that pore have a shape like tabular more than PH1 and PH2. This value may affect from the fracture pores in PH3 sample.

PH1 3D Pore Shape and Volume



PH2 3D Pore Shape and Volume



PH3 3D Pore Shape and Volume

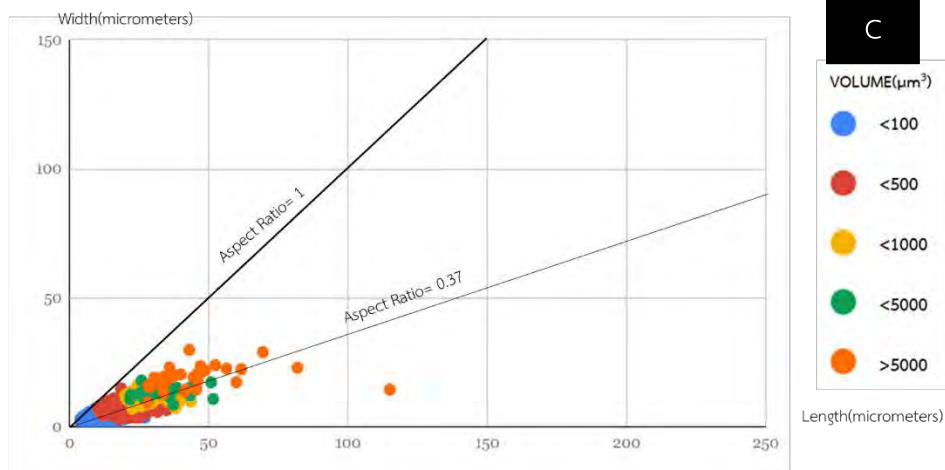


Figure 4.7 Width versus Length plot of pore in PH1, PH2, and PH3

4.4 Pore Throat

Pore throat is an intergranular rock, the small pore space at the point where two grains meet (Figure 1.5), which connects two larger pore volumes. The number, size and distribution of the pore throats control many of the resistivity, flow and capillary-pressure characteristics of the rock (Schlumberger Oilfield Glossary, 2015). This study will focus on shape, size, and connectivity of pore throat. Auto skeleton module is used to model the connectivity of pore (Figure 4.8) and then calculate the geometry of connectivity area in term of width, length, radius, and volume (Figure 4.9). The geometry of connectivity area is identified to be pore throat and re calculate to show the specific character of throat shape inside the rock.

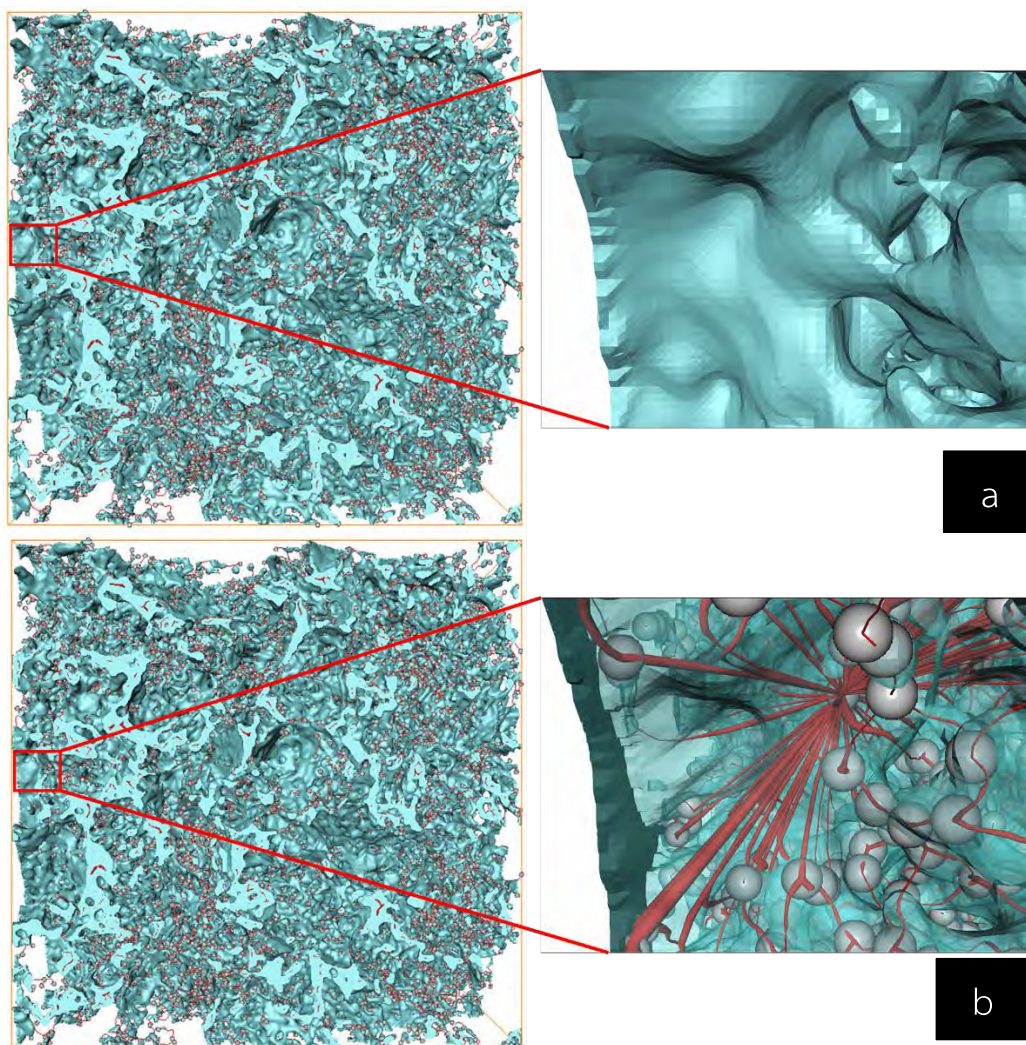


Figure 4.8 Pore Skeleton use to identify and calculate geometry of pore throat. (a) Cyan areas represent the whole pore space in sample after Auto Skeleton Module (b) Grey spheres represent the pore chamber and red skeleton represent the connectivity area of pore chamber (pore throat)

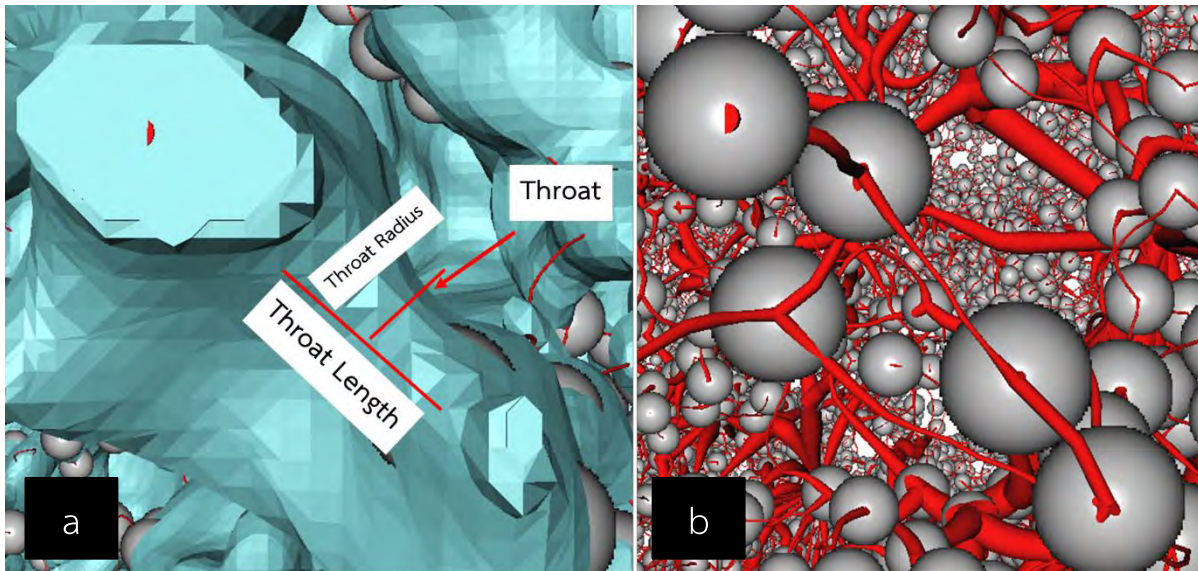


Figure 4.9 (a) 3D simulation of Pore Throat show the radius and length which can calculate the geometry of throat. (b) Grey spheres represent the pore chamber and red skeleton represent the connectivity area of pore chamber (pore throat)

The result show that the greatest ranges of pore throat radius are between 0.36 to 1.44 μm (Table 4.1 and Figure 4.10). The biggest pore throat size is pore throat in PH3, the second is PH1 and the last one is PH2. PH2 sample no show in pore throat size over 1.44 μm .

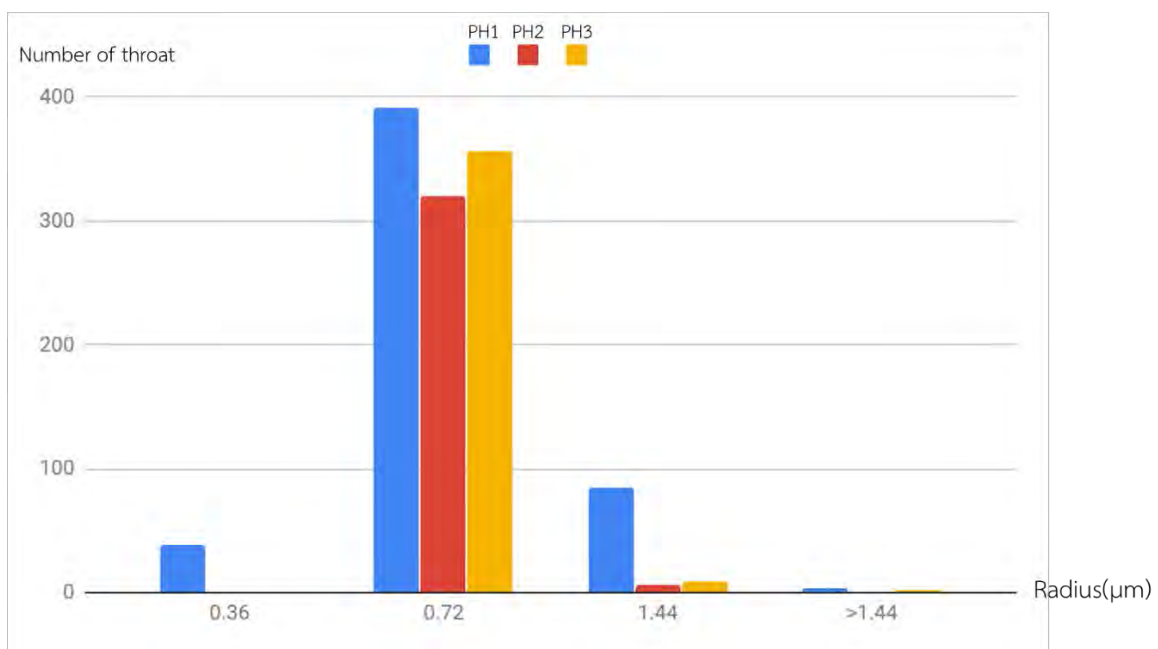


Figure 4.10 This graph shows pore throat radius of PH1, Ph2, and PH3

	Minimum radius (μm)	Maximum radius (μm)	Average (μm)
PH1	0.36	1.74	0.51
PH2	0.41	0.87	0.48
PH3	0.39	2.67	0.56

Table 4.1 Minimum, maximum, average radius of pore throat in PH1, PH2. And PH3

Width, length, and radius of pore throat will turn into Intermediate length(I), longest length(L) and shortest length(S) respectively. Then the ratio between S/I and I/L will plot on Zingg Diagram (Zingg,1935) (Figure4.11) to observe the shape of throat that evaluate the porosity and permeability. The simple rule is ($L \geq I \geq S$) when the type of shape will be spheroid ($L \approx I \approx S$), blade ($L \gg I > S$), rod ($L > I \approx S$), and discoid ($L \approx I \gg S$).

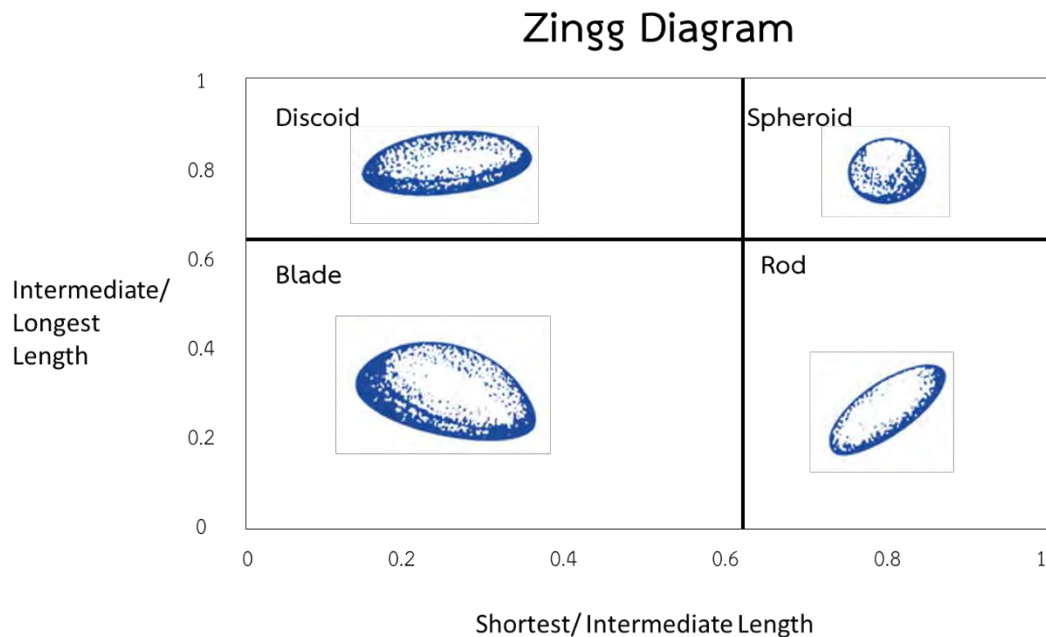


Figure 4.11 The Zingg diagram (Illustrated from Zingg, 1935)

Figure 4.12 shows the results of Zingg diagram plot in PH1, PH2, and PH3. PH1 contains amount of Rod, Spheroid, Blade, and discoid pore throat shape respectively. In the PH2 show the result like the PH1 but the number of Blade and Discoid shape is more than in PH1 this may affect from the number of pores at the edge of rigid grains in PH2. Furthermore, PH3 contains only Rod and Spheroid pore throat shape where the greatest type of pore throat is Rod shape. This may affect from the natural shape of pore fracture which dominated in PH3 that generally are the tabular or flat.

4.5 Porosity and Permeability

The results of porosity and permeability show in Table 4.2. The porosity in each sample have a reasonable relationship between pore volume in 4.3 and porosity as shown in Figure 4.13. PH1 contain the PH1-2, PH1-2, and PH1-3 VOI. PH1-1, PH1-2, and PH1-3 have porosity 14.5, 9.41, 14.03% and permeability 0.23, 0.14, and 0.19 mD respectively. The porosity in PH1 have direct variation with permeability. The average porosity is 12.65% and average permeability is 0.19 mD. Porosity and permeability of PH1 is in the second order of all samples.

PH2-1, PH2-2, and PH2-3 have porosity 12.7, 11.35, 10.35% and permeability 0.17, 0.18, and 0.12 mD respectively. The porosity in PH2 have direct variation with permeability. The average porosity is 11.47% and average permeability is 0.16 mD. Porosity and permeability of PH1 is in the third order of all samples.

PH3-1, PH3-2, and PH3-3 have porosity 13.31, 15.86, 24.34% and permeability 0.14, 0.27, and 0.49 mD respectively. The porosity in PH3 have direct variation with permeability but have the spread of data in PH3-3 due to the number of pores fractures in this sample. The average porosity is 11.47% and average permeability is 0.16 mD. Porosity and permeability of PH1 is in the first order of all samples.

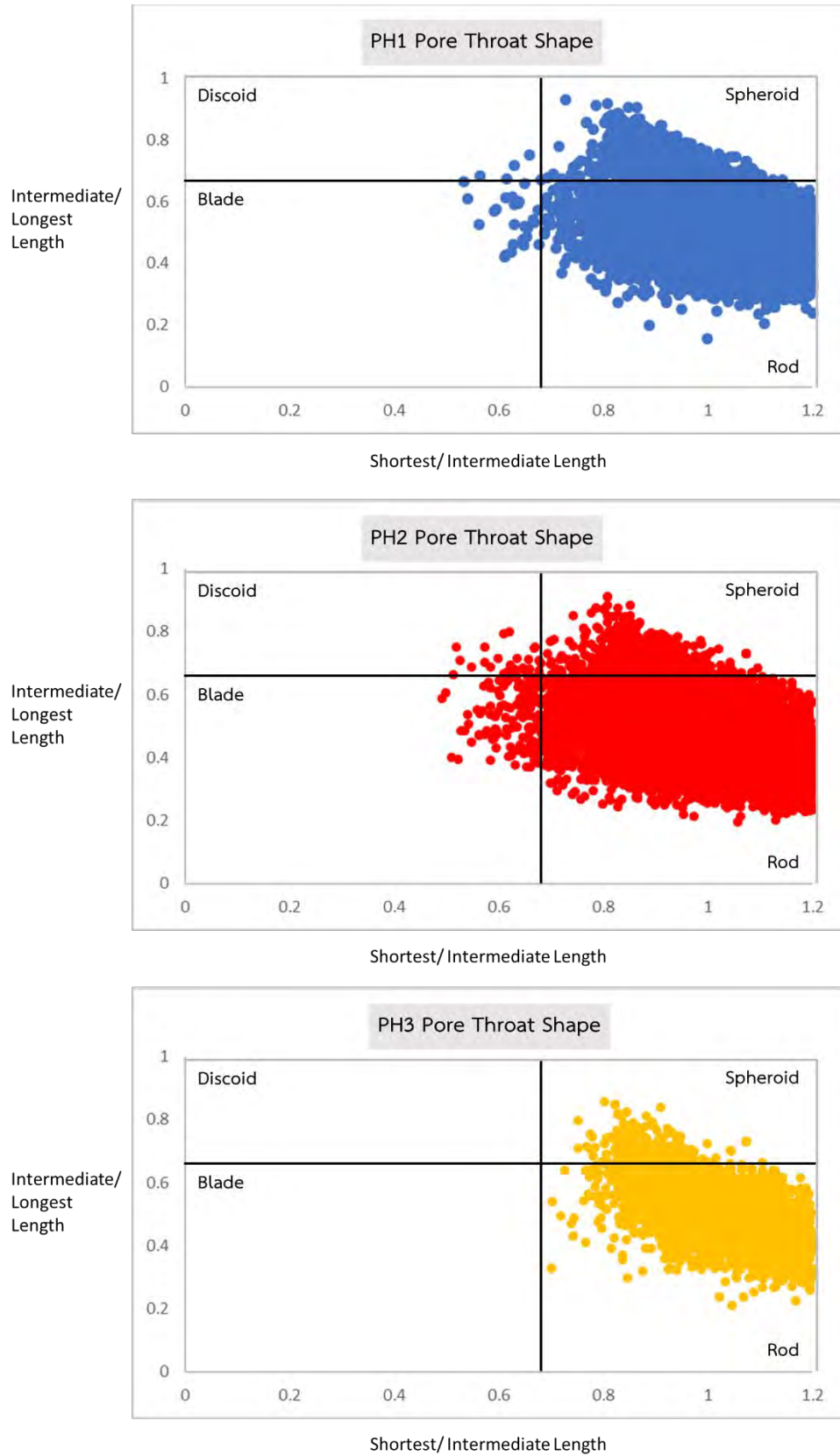


Figure 4.12 Zingg diagram plot of I,L, S length of pore throat in PH1, PH2, and PH3

	Porosity (%)	Permeability (mD)
PH1-1	14.5	0.23
PH1-2	9.41	0.14
PH1-3	14.03	0.19
Average (SD)	12.65 (2.81)	0.19 (0.05)
PH2-1	12.7	0.17
PH2-2	11.35	0.18
PH2-3	10.35	0.12
Average (SD)	11.47 (1.18)	0.16 (0.03)
PH3-1	13.31	0.14
PH3-2	15.86	0.27
PH3-3	24.34	0.49
Average (SD)	17.84 (5.77)	0.30 (0.18)

Table 4.2 Porosity and Permeability of PH1, PH2, and PH3

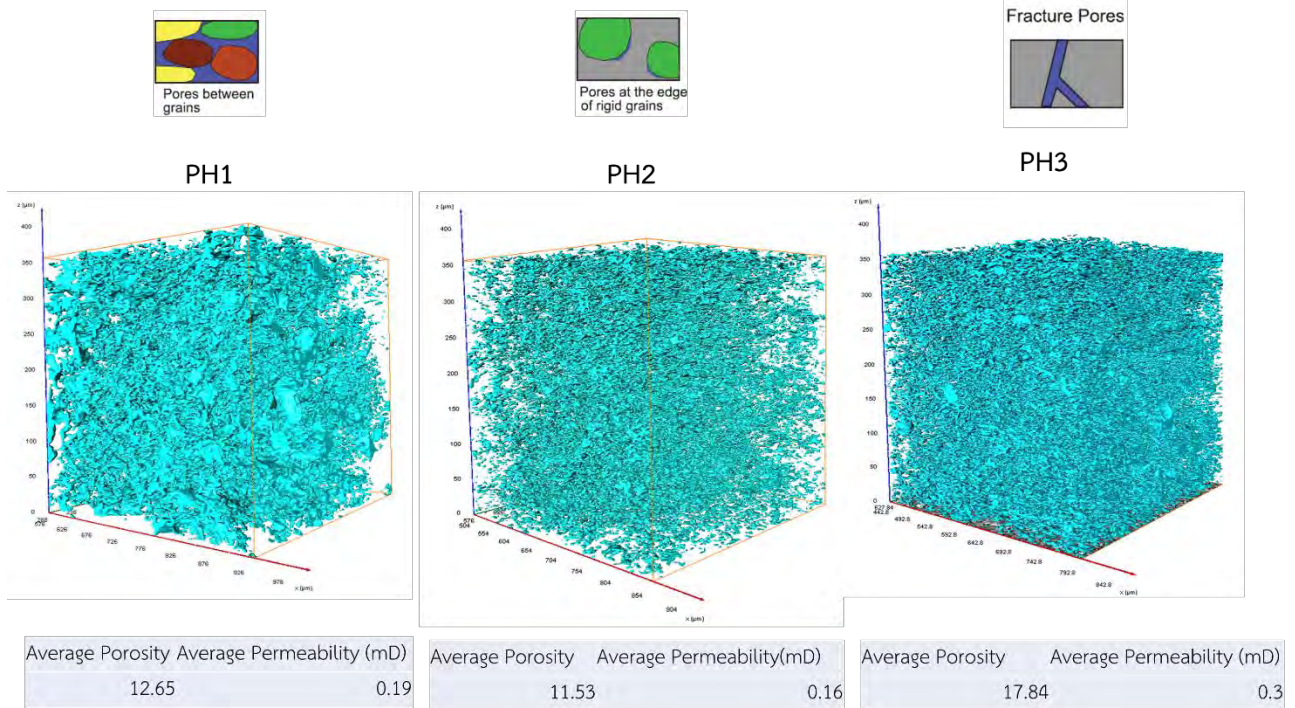


Figure 4.13 3D pore distribution in PH1, PH2, and PH3

Chapter V

Discussion and Conclusion

5.1 Porosity and Permeability

Porosity in all sample are ranging from 9.41 % to 34.34 % and permeability are ranging from 0.12 to 0.49 mD. Figure 4.14 shows the plot between porosity and permeability this have a linear variation of data mean that the higher porosity the higher permeability. Each porosity values are in the range and more than the standard cut off which porosity of tight sandstone reservoir should be average value near 10% porosity and less than 1 mD of permeability these values are officially recognized by the U.S. Federal Energy Regulatory Commission (FERC). When compare the porosity and permeability in the tight sandstone in study of Zou et al, 2010, the permeability of tight sandstone reservoir is usually less than 0.1 mD. Due to the pores in tight sandstone reservoirs in most Chinese basins are characterized by intergranular and intragranular dissolution pore types which show narrow and less effective pore throat, poor pore size distribution and overall poor reservoir quality. This reason effects the higher permeability observes in tight sandstone in Phitsanulok basin which have wide pore and amount of effective pore throat.

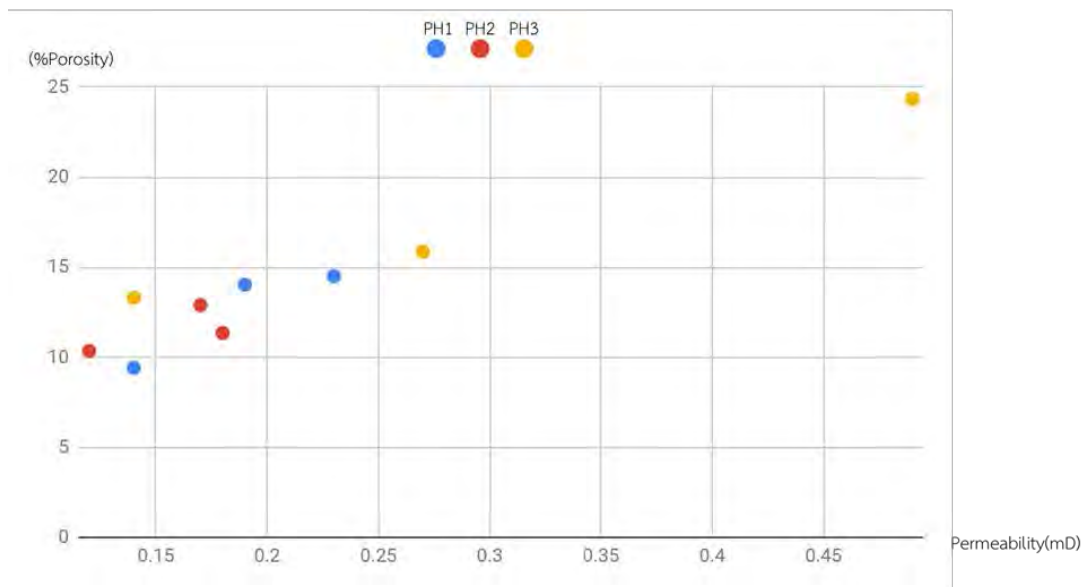


Figure 4.14 Porosity versus Permeability plot of 9 VOI

5.2 Pore Classification

PH1 samples have a second ranks of average porosity and permeability which relate to the volume of pore inside the whole sample that higher than PH2 but lower than PH3. This permeability and porosity in PH1 due to the pore between grains that dominated in PH1 sample. For PH2, the lowest porosity and permeability may affect from the quantity of pore at the edge of rigid grains and the volume of pore in this sample shows the smaller volume than the other samples. PH3 have high porosity and permeability that affect from the high volume of pore are shows in the sample. Not only the volume but also the greatest numbers of fractures pore that dominated only in the PH3 is the factors that enhances the porosity and permeability in the sample (Figure 4.13). The fracture pores contain high connectivity of pore shape so the higher permeability in the rocks with this pore type while the pore at the edge of rigid grains show low connectivity and effect to the permeability in the rocks. For study of tight sandstone by Zou et al in 2015 show that the secondary pore or fracture pore are the importance character of tight gas sandstone reservoir in most of Chinese Basin.

5.3 3D aspect ratio and pore throat

3D aspect ratio of pore show that all samples contain high elongation of pore size so the elongation of pore effect the high connectivity of each pore chamber which enhance the ability of fluid flow in rock unit. For throat classification, throat radius of all sample are 0.36 to 2.67 μm when compare to the throat diameter in the study of diameters in siliciclastic rocks (Nelson, 2009) found that the throat from three sample in Phitsanulok basin are in the range of tight sandstone reservoir because usually the pore throat in sandstone reservoirs is 20 μm while tight sandstone is 2 μm . The ranges of diameters are like to the sandstone in East Texas Basin (Figure 4.15). The plot between pore and pore throat diameters with the grain size (Figure 4.16) which compared to 26 sandstone samples worldwide. The samples in this study are in the range of tight sandstone range that can evaluate to be the reservoir. From the result shows some smaller throat observes in sample in this study when compare to the sandstone sample in Nelson's study. This may affect from the method used which is mercury injection that can detect the size of object bigger than detection from Synchrotron X-ray tomography.

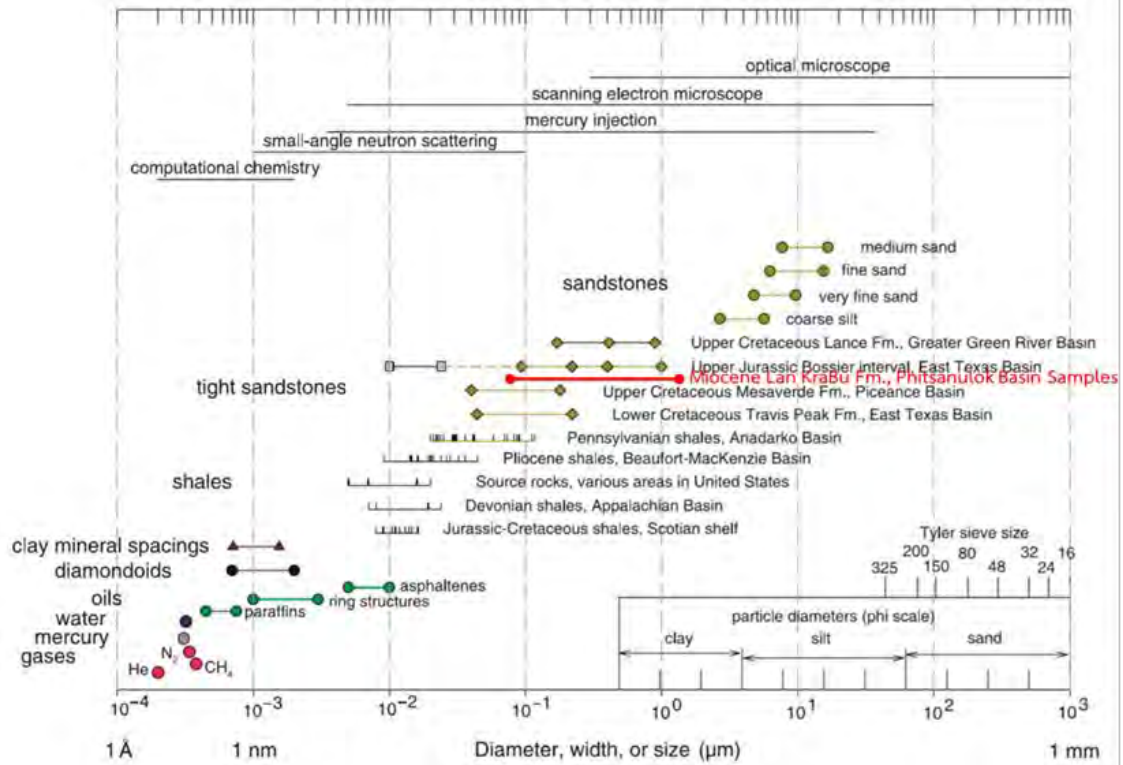


Figure 4.15 Sizes of pore throats in siliciclastic rocks on a logarithmic scale covering seven orders of magnitude. The red line shows the pore throat size ranges of 9 VOI of this study (Modified from Nelson, 2009)

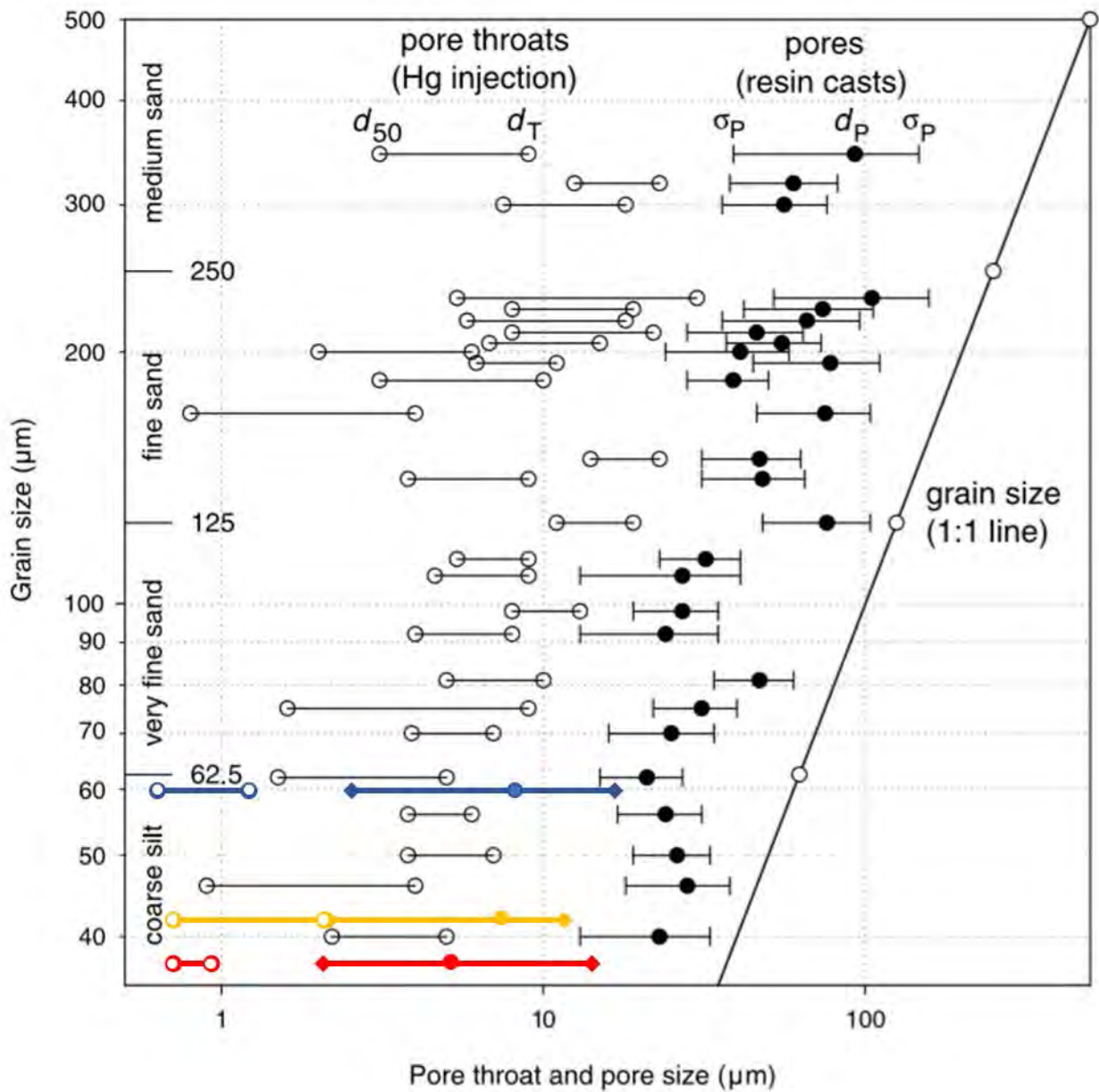


Figure 4.16 Grain size, pore size, and pore-throat size for 27 sandstone samples (Wardlaw and Cassan, 1979) The blue, red, and yellow line show the pore and pore throat of PH1, PH2, and PH3 respectively.

5.4 Conclusion

Porosity range are from 9.41 to 24.34 % and Permeability range are from 0.12 to 0.49 mD which can be the tight sandstone reservoir. Most of pore types are interparticle pore (pore between grains and pore at the edge of rigid grains) and fracture pore can enhance the highest permeability and porosity in sample. Pore throat size range from 0.36 to 2.67 μm which have the range in the tight sandstone and the diameter range are likely to sandstone in East Texas Basin. Most of pore throat shape is rod type spheroid type that the longer of shape the more permeability in sample. PH3 samples have highest porosity and permeability. The second is PH1 and the last is PH2 the flow simulation PH3 compare to PH2 are show in Figure 4.17

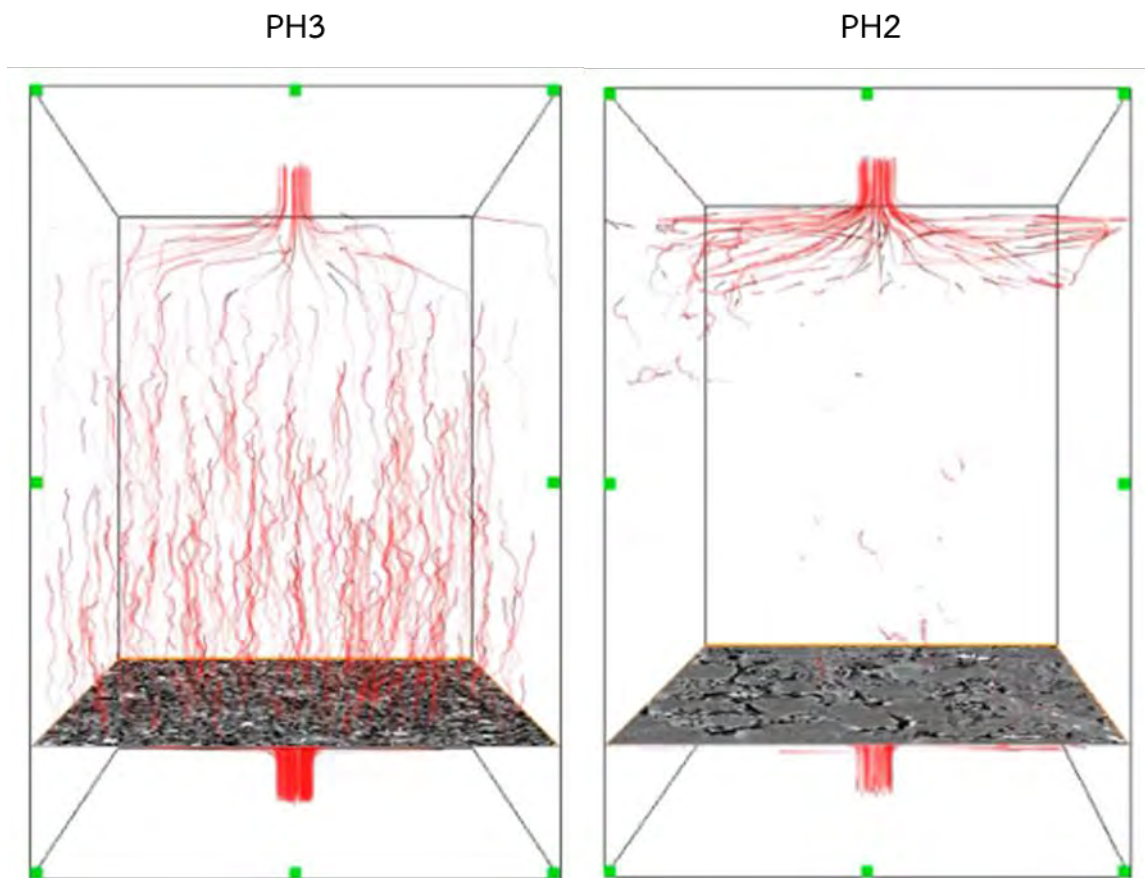


Figure 4.17 Flow simulation PH3 compare to PH2

References

- Ainsworth, B. et al., 1997. Sirikit Field Review 1997 Part 2 Geology. Internal Report of Invervation of Thai Shell Exploration and Production.
- Bal, A.A. et al., 1992. The Tertiary Phitsanulok Lacustrine Basin, Thailand, eds. National Conference on "Geologic Resources of Thailand: Potential For Future Development", 247-258. Bangkok:
- C&C Reservoirs. "Sirikit - Reservoir Evaluation Report Far East Sirikit..." The Logistic Model Has Good and Bad Features PROS CONS Mathematically Tractable Web.
- Dyman, T., & Schmoker, J. (1997). Comparison of natural gas assessments. *Open-File Report*.
- Glemser C. Petrophysical and geochemical characterization of Middle carbonates from the Weyburn oilfield using synchrotron X-ray computed microtomography. Weyburn Oilfield. 2008
- Kanitpanyacharoen, W., Parkinson, D. Y., Carlo, F. D., Marone, F., Stampanoni, M., Mokso, R., . . . Wenk, H. (2012, 11). A comparative study of X-ray tomographic microscopy on shales at different synchrotron facilities: ALS, APS and SLS. *Journal of Synchrotron Radiation*, 20(1), 172-180. doi:10.1107/s0909049512044354
- Kets, F., Kanitpanyacharoen, W., Wenk, H., & Wirth, R. (2012, 01). Preferred Orientation, Microstructures, and Porosity Analysis of Posidonia Shales. *3rd EAGE Shale Workshop - Shale Physics and Shale Chemistry*. doi:10.3997/2214-4609.20143937
- Kiatrable, T., Noosri, R., Hamdan, M. K., Kusolsong, S., Palviriyachote, S., Suwatjanapornphong, S., . . . Press, D. (2016). Application of Geomechanics for Tight Oil Reservoir Characterisation and Field Development. *International Petroleum Technology Conference*. doi:10.2523/iptc-18833-ms
- Lai, J., Wang, G., Wang, Z., Chen, J., Pang, X., Wang, S., . . . Fan, X. (2018, 02). A review on pore structure characterization in tight sandstones. *Earth-Science Reviews*, 177, 436-457. doi: 10.1016/j.earscirev.2017.12.003
- Loucks, R. G., Reed, R. M., Ruppel, S. C., & Hammes, U. (2012, 06). Spectrum of pore types and networks in mudrocks and a descriptive classification for matrix-related mudrock pores. *AAPG Bulletin*, 96(6), 1071-1098. doi:10.1306/08171111061

- Nelson, P. H. (2009, 03). Pore-throat sizes in sandstones, tight sandstones, and shales. *AAPG Bulletin*, 93(3), 329-340. doi:10.1306/10240808059
- Pinyo, Komon, 2011, Unconventional petroleum system evaluation of the Chum Saeng Formation, Phitsanulok Basin, Thailand, in International Conference on Geology, Geotechnology, and Mineral Resources of Indochina [GEOINDO]: 11th Khon Kaen, Thailand, December 1–3, 2001, Proceedings, Khon Kaen University, Faculty of Technology, Department of Geotechnology, p. 267–280
- “Pore Throat.” *Pore Throat - Schlumberger Oilfield Glossary*,
www.glossary.oilfield.slb.com/en/Terms/p/pore_throat.aspx.
- Proposals - APEC Unconventional Gas Census: Evaluating...*,
aimp2.apec.org/sites/PDB/Lists/Proposals/DispForm.aspx?ID=608.
- “Tight Gas Reservoirs: Evaluation.” *Tight Gas Reservoirs: Evaluation - AAPG Wiki*,
wiki.aapg.org/Tight_gas_reservoirs:_evaluation.
- Zhenpeng, L., Weifeng, L., Desheng, M., Qingjie, L., Ninghong, J., Tong, L., . . . Danyong, L. (2015). Characterization of Pore Structure in Tight Oil Reservoir Rock. *SPE/IATMI Asia Pacific Oil & Gas Conference and Exhibition*. doi:10.2118/176358-ms
- Zou, C., Zhu, R., Liu, K., Su, L., Bai, B., Zhang, X., . . . Wang, J. (2012, 06). Tight gas sandstone reservoirs in China: Characteristics and recognition criteria. *Journal of Petroleum Science and Engineering*, 88-89, 82-91. doi: 10.1016/j.petrol.2012.02.001